H．知的所有権の出願・登録状況

1．特許取得

なし

2．実用新案登録

なし

3.その他

別紙３

厚生労働科学研究費補助金（第３次対がん総合戦略研究事業）
分担研究報告書

チロシンホスファターゼの異常と発がん、浸潤・転移

分担研究者　的崎　尚　　神戸大学大学院医学研究科　シグナル統合学分野　教授

研究要旨　　チロシンリン酸化シグナルの制御には、チロシンキナーゼと共にチロシンホスファターゼ(PTP)が重要である。しかし、PTP の異常が発がんやがんの浸潤・転移にどのように関わっているかについては不明の点が多い。大腸がんの発生を促進的に制御する可能性のある受容体型 PTP である SAP-1 について、SAP-1 の脱チロシンリン酸化基質が膜型糖化分子 pp90 であることを見出した。この分子は、腸上皮細胞に特異的に発現し微絨毛に局在する。また、細胞内領域が Src によりチロシンリン酸化をうけ、その強制発現は複数のシグナル分子を活性化する。白血病で遺伝子異常が検出される PTP である Shp2 の結合分子 SIRPα はマクロファージによる貪食を抑制的に調節している。この性質を利用して、SIRPα機能を人為的に操作することにより、ADCC 活性を有するがんの分子標的薬の効果を増強する、あるいは浸潤・転移を抑制する新たな抗がん剤を開発できる可能性を示すことが出来た。

Ａ．研究目的

チロシンリン酸化シグナルは、生理的な細胞の増殖・分化・運動の制御に重要なシグナル系であり、一方、がんの発生、浸潤・転移の分子機構にこのシグナル系の異常が深く関与していることが示されている。チロシンリン酸化シグナルの制御には、チロシンキナーゼと共にチロシンホスファターゼ(PTP)が重要であるが、PTPの異常が発がんやがんの浸潤・転移にどのように関わっているかについては未だ不明な点が多い。分担研究者が見出した受容体型PTPであるSAP-1は、ヒト胃がんや大腸がんに高度に発現するPTPであり、大腸がんモデルにおいて、SAP-1ががんの発生を促進的に制御することを見出している。一方、SAP-1は腸上皮細胞の微絨毛に特異的に発現するがその生理機能は未だ不明である。そこで、本研究では、SAP-1の生理機能と発がんにおける役割を明らかにすることを目的とする。また、細胞質型PTPであるShp2は増殖因子によるRasの活性化に重要であることが知られており、最近では、Shp2の活性型遺伝子変異がNoonan症候群と呼ばれる遺伝疾患やそれに随伴するAMLやMDSなどの血液系腫瘍の原因として見出され注目されている。分担研究者はShp2の結合分子として受容体型分子SIRPαを見出しているが、がんにおける役割は不明である。すでに、SIRPαを高度に発現するヒトメラノーマ細胞のin vitroでのmigrationを抗SIRPα抗体が抑制することを明らかにしている。また、SIRPαはマクロファージに強く発現しており、標的細胞上のリガンド分子であるCD47がSIRPαに結合するとマクロファージによる貪食を負に制御することが知られている。そこで、前年度、マウス悪性黒色腫細胞株（B16メラノーマ）接種による肺転移モデルにおいて、ADCC活性を有する抗メラノーマ特異的抗体による腫瘍排除を検討したところ、SIRPα遺伝子破壊(KO)マウスにおいて腫瘍排除が顕著に増強していることを見出した。そこで、本年度はさらに、CD47-SIRPα系を利用した、新たながん治療法開発の基礎的検討を行った。

Ｂ．研究方法

(1) 前年度、SAP-1 の脱チロシンリン酸化基質分子として同定していた pp90 のモノクローナル抗体を作製し、組織分布や細胞内局在を検討した。また、pp90 の細胞内のチロシンリン酸化に重要な分子ならびに結合分子の探索を行った。さらに、培養細胞に強制発現した際のシグナル分子の挙動につき解析をした。

(2) 前年度に引き続き、B16 メラノーマ接種による肺転移モデルを用いて、抗体依存性の細胞障害（ADCC）活性を有する抗メラノーマ特異的抗体(TA99)による腫瘍排除を検討すると共に、抗 SIRPα抗体単独あるいは TA99 との併用による腫瘍排除の効果を検討した。

Ｃ．研究結果

(1) SAP-1の脱チロシンリン酸化基質分子pp90の

組織発現を検討したところ、腸管に特異的に発現し、さらに腸上皮細胞の微絨毛に局在することが明らかとなった。また、pp90の細胞内領域のチロシンリン酸化には、細胞質型チロシンキナーゼのSrcやFynが重要であり、SAP-1の強制発現により脱リン酸化されることが分かった。さらに、pp90の強制発現により、MAPキナーゼの活性化や複数のシグナル分子のチロシンリン酸化が誘導されることが明らかとなった。

(2) マウスB16メラノーマにおいても、SIRPαが高度に発現することを確認した。そこで、B16メラノーマ接種による肺転移モデルにおいて抗SIRPα抗体単独の効果を検討した結果、有意に肺転移を抑制することが分かった。また、ADCC活性を有する抗メラノーマ特異的抗体TA99との併用による腫瘍排除の効果を検討したところ、有意な相乗効果が観察された。現在、この機序につき細胞特異的SIRPα KOマウスなどを用いて検討中である。

D．考察

SAP-1はヒト胃がんや大腸がんに高度に発現するPTPであり、大腸がんモデルにおいてSAP-1ががんの発生を促進的に制御することを見出していたが、その分子基盤は不明であった。すでに、SAP-1の脱チロシンリン酸化基質として膜貫通型糖化分子であるpp90を同定しており、今年度はこのpp90の性状を詳細に解析した。pp90は腸上皮細胞に高度に発現し微絨毛に局在することから、この分子がin vivoにおけるSAP-1の脱チロシンリン酸化基質である可能性がより高まった。また、pp90のチロシンリン酸化の機序や下流の細胞内シグナルが一部明らかとなった。今後は、pp90の生理機能やSAP-1による発がん機序への関与につき検討する必要がある。すでに、SIRPα KO マウスにおいて抗メラノーマ特異的抗体による腫瘍排除が顕著に増強することを見出しており、抗SIRPα抗体を用いてCD47-SIRPα結合を阻害することで、ADCC活性を有する分子標的薬の効果増強の可能性が示唆された。今回、抗SIRPα抗体単独でも、メラノーマの肺転移を抑制したことから、抗SIRPα抗体が２つの異なる機序を介したがん治療薬として利用できる可能性が考えられた。今後、抗SIRPα抗体単独の効果が、この抗体自体が誘導するADCC活性を介したものであるか否か、あるいはがん細胞のmigrationを抑制し転移の過程を阻害しているかなどにつき、in vitro系における検討が必要である。

E．結論

本研究により、受容体型PTPであるSAP-1の作用機構に新規膜型分子であるpp90が関与する可能性が示唆された。また、Shp2の結合分子であるSIRPαの機能を人為的に操作することにより、がんの分子標的薬として利用できる可能性が示された。

G．研究発表

1．論文発表

Iwamura H, Saito Y, Sato-Hashimoto M, Ohnishi H, Murata Y, Okazawa H, Kanazawa Y, Kaneko T, Kusakari S, Kotani T, Nojima Y, Matozaki T. Essential roles of SIRPα in homeostatic regulation of skin dendritic cells. Immunol Lett, 135: 100-107, 2011.

Sato-Hashimoto M, Saito Y, Ohnishi H, Iwamura H, Kanazawa Y, Kaneko T, Kusakari S, Kotani T, Mori M, Murata Y, Okazawa H, Ware CF, Oldenborg P-A, Nojima Y, Matozaki T. Signal regulatory protein α regulates the homeostasis of T lymphocytes in the spleen. J Immunol, 187: 291-297, 2011.

Verjan Garcia N, Umemoto E, Saito Y, Yamasaki M, Hata E, Matozaki T, Murakami M, Jung YJ, Woo SY, Seoh JY, Jang MH, Aozasa K, Miyasaka M. SIRPα/CD172a regulates eosinophil homeostasis. J Immunol, 187: 2268-2277, 2011.

Zhao X, van Beek EM, Schornagel K, van der Maaden, H, van Houdt M, Otten MA, Finetti P, van Egmond M, Matozaki T, Kraal G, Birnbaum D, van Elsas A, Kuijpers TW, Bertucci F, van den Berg TK. CD47-signal regulatory protein-α (SIRPα) interactions form a barrier for antibody-mediated tumor cell destruction. Proc Natl Acad Sci USA, 108: 18342-18347, 2011.

H．知的所有権の出願・登録状況

1. 特許取得

なし

2. 実用新案登録

なし

3.その他

なし

別紙４

研究成果の刊行に関する一覧表

雑誌

発表者氏名	論文タイトル名	発表誌名	巻号	ページ	出版年
Satow R, Shitashige M, Jigami T, Fukami K, Honda K, Kitabayashi I, Yamada T.	β -catenin inhibits promyelocytic leukemia protein tumor suppressor function in colorectal cancer cells.	Gastroenterology	142	572-581	2012
Iwanami A, Gini B, Zanca C, Matsutani T, Assuncao A, Nael A, Dang J, Yang H, Zhu S, Kohyama J, Kitabayashi I, Cavenee WK, Cloughesy TF, Furnari FB, Nakamura M, Toyama Y, Okano H, Mischel PS.	PML mediates glioblastoma resistance to mammalian target of rapamycin (mTOR)-targeted therapies.	Proc Natl Acad Sci USA	110	4339-4344	2013
Rokudai S, Laptenko O, Arnal SM, Taya Y, Kitabayashi I, Prives C.	MOZ increases p53 acetylation and premature senescence through its complex formation with PML.	Proc Natl Acad Sci USA	110	3895-3900	2013
Yasuda T, Hayakawa F, Kurahashi S, Sugimoto K, Minami Y, Tomita A, Naoe T.	B Cell Receptor-ERK1/2 Signal Cancels PAX5-Dependent Repression of BLIMP1 through PAX5 Phosphorylation: A Mechanism of Antigen-Triggering Plasma Cell Differentiation.	J Immunol.	188	6127-6134	2012
Hayakawa F, Sugimoto K, Kurahashi S, Sumida T, Naoe T.	GATA2 zinc finger 2 mutation found in acute myeloid leukemia impairs myeloid differentiation.	Leukemia Rsearch Reports	2	21-25	2013
Kikushige Y, Akashi K.	TIM-3 as a therapeutic target for malignant stem cells in acute myelogenous leukemia.	Ann N Y Acad Sci	1266	118-12	2012
Kuriyama T, Takenaka K, Kohno K, Yamauchi T, Daitoku S, Yoshimoto G, Kikushige Y, Kishimoto J, Abe Y, Harada N, Miyamoto T, Iwasaki H, Teshima T, Akashi K.	Engulfment of hematopoietic stem cells caused by down-regulation of CD47 is critical in the pathogenesis of hemophagocytic lymphohistiocytosis.	Blood	120	4058-4067	2012
Kaneko T, Saito Y, Kotani T, Okazawa H, Iwamura H, Sato-Hashimoto M, Kanazawa Y, Takahashi S, Hiromura K, Kusakari S, Kaneko Y, Murata Y, Ohnishi H, Nojima Y, Takagishi K, Matozaki T.	Dendritic cell-specific ablation of the protein tyrosine phosphatase Shp1 promotes Th1 cell differentiation and induces autoimmunity.	J Immunol	188	5397-5407	2012
Alenghat FJ, Baca QJ, Rubin NT, Pao LI, Matozaki T, Lowell CA, Golan DE, Neel GB, Swanson KD.	Macrophages require Skap2 and Sirpα for integrin-stimulated cytoskeletal rearrangement.	J Cell Sci	125	5535-5545	2012

van Beek EM, Zarate JA, van Bruggen R, Schornagel K, Tool ATJ, Matozaki T, Kraal G, Roos D, van den Berg TK.	SIRPa controls the activity of the phagocyte NADPH oxidase by restricting the expression of $gp91^{phox}$.	Cell Report	2	748-755	2012
Marschinke F, Hashemian S, Matozaki T, Oldenborg P-A, Strömberg I. The absence of CD47 promotes nerve fiber growth from cultured ventral mesencephalic dopamine neurons.	The absence of CD47 promotes nerve fiber growth from cultured ventral mesencephalic dopamine neurons.	PLos ONE	7	e45218	2012

GASTROENTEROLOGY 2012;142:572–581

β-Catenin Inhibits Promyelocytic Leukemia Protein Tumor Suppressor Function in Colorectal Cancer Cells

REIKO SATOW,*,‡ MIKI SHITASHIGE,* TAKAFUMI JIGAMI,* KIYOKO FUKAMI,‡ KAZUFUMI HONDA,* ISSAY KITABAYASHI,§ and TESSHI YAMADA*

*Divisions of *Chemotherapy and Clinical Research and §Hematological Malignancy, National Cancer Center Research Institute, Tokyo; and ‡Laboratory of Genome and Biosignal, Tokyo University of Pharmacy and Life Sciences, Tokyo, Japan*

BACKGROUND & AIMS: Loss of promyelocytic leukemia protein (PML) nuclear body (NB) formation has been reported in colorectal and other solid tumors. However, genetic alteration of *PML* is rarely observed in these tumors; the exact mechanisms that mediate loss of PML function are not known. **METHODS:** We previously used a comprehensive shotgun mass spectrometry approach to identify PML as 1 of 70 proteins that coimmunoprecipitate with anti–T-cell factor 4 in DLD-1 and HCT116 colorectal cancer cell lines; we investigated the effects of altered β-catenin expression on PML function in these cells. **RESULTS:** β-catenin specifically interacted with the product of *PML* transcript variant IV (PML-IV) through the armadillo repeat domain of β-catenin. Overexpression of β-catenin in colorectal cancer cells disrupted the subcellular compartmentalization of PML-IV, whereas knockdown of β-catenin restored formation of PML-NB. Modification of PML by the small ubiquitin-related modifier (SUMO) is required for proper assembly of PML-NB. β-catenin inhibited Ran-binding protein 2–mediated SUMOylation of PML-IV. **CONCLUSIONS: β-catenin interacts with PML isoform IV and disrupts PML-IV function and PML-NB formation by inhibiting Ran-binding protein 2–mediated SUMO modification of PML-IV. These findings indicate the involvement of a posttranslational mechanism in disruption of PML-NB organization in cancer cells and provide more information about the oncogenic functions of β-catenin.**

Keywords: Wnt Signaling; Colorectal Cancer; TCF4; PML.

BASIC AND TRANSLATIONAL AT

The majority of colorectal cancers have somatic mutations in the adenomatous polyposis coli (*APC*) gene, and about one-half of those with the wild-type *APC* gene have mutations in the β-catenin (*CTNNB1*) gene.[1–3] Either mutation results in stabilization and accumulation of β-catenin protein. It is believed that accumulated β-catenin exerts its oncogenic function mainly by cotransactivating the target genes of TCF/lymphoid enhancer factor (LEF)-family transcriptional factors.[4] However, β-catenin is a multifunctional protein, and its function varies according to the context of partner proteins with which it forms complexes.[5] Our recent series of proteomics studies has revealed that β-catenin plays various roles in DNA damage recognition,[6,7] pre-messenger RNA splicing,[8,9] and cell motility[10] through interaction with poly (adenosine diphosphate–ribose) polymerase-1, Ku70, FUS/TLS proto-oncogene product, splicing factor 1, and actinin 4.

A previous unbiased analysis of the protein composition of the T-cell factor (TCF) 4 and β-catenin nuclear complex we performed using highly tuned mass spectrometry identified 70 proteins,[11] among which promyelocytic leukemia protein (PML) attracted our current attention. PML is a tumor suppressor that was originally identified in the t(15;17) chromosome translocation site of acute promyelocytic leukemia. This chromosome translocation generates the PML and retinoic acid receptor α fusion protein,[12,13] which acts as a dominant negative mutant for PML and inhibits its tumor suppressor function.[14–16] PML is essential for the formation of the nuclear speckled substructure known as PML-nuclear body (NB). PML recruits a large variety of proteins into PML-NB and mediates various fundamental nuclear functions such as DNA replication, transcription, and epigenetic silencing,[17–22] as well as regulating cell death, proliferation, and senescence.[14,17,19,23,24] Inhibition of PML-NB formation has been considered one of the main mechanisms by which the PML–retinoic acid receptor α fusion protein promotes leukemogenesis.

Loss of the tumor-suppressive function of PML does not seem to be limited to hematologic malignancies. Formation of PML-NB and expression of PML protein are often lost in various human solid tumors including colorectal cancer,[25,26] but mutation or loss of heterozygosity of the *PML* gene has rarely been detected, and expression of PML messenger RNA is well retained in these tumors, indicating that the disruption of PML function is not caused by genetic or epigenetic inactivation of *PML*. However, the precise molecular mechanisms behind the loss of PML function in solid tumors have remained largely unknown.

Here we report the novel posttranslational regulation of PML tumor suppressor function by an oncogene product,

Abbreviations used in this paper: DAPI, 4′,6-diamidino-2-phenylindole; GST, glutathione S-transferase; HA, hemagglutinin; HDAC7, histone deacetylase 7; NB, nuclear body; PML, promyelocytic leukemia protein; RanBP2, Ran-binding protein 2; SDS-PAGE, sodium dodecyl sulfate/polyacrylamide gel electrophoresis; siRNA, small interfering RNA; SUMO, small ubiquitin-related modifier; TCF, T-cell factor.

© 2012 by the AGA Institute
0016-5085/$36.00
doi:10.1053/j.gastro.2011.11.041

β-catenin. β-catenin physically interacts with PML and inhibits the SUMOylation of PML and subsequent formation of PML-NB. Our data reveal a new aspect of β-catenin function and may provide insights into the molecular mechanisms of colorectal carcinogenesis, as well as suggesting novel forms of therapeutic intervention.

Materials and Methods

Cell Lines

The human embryonic kidney cell line HEK293 and the human colorectal cancer cell lines *DLD1* and *Lovo* were obtained from the Health Science Research Resources Bank (Osaka, Japan). The human colorectal cancer cell line SW48 was purchased from American Type Culture Collection (Rockville, MD). The human cervical cancer cell line HeLa was obtained from Riken Cell Bank (Tsukuba, Japan). Mitomycin C was purchased from Sigma-Aldrich (St Louis, MO).

Plasmids and Small Interfering RNA

pLNCX constructs encoding Flag-tagged human PML isoforms (Flag-PML-I to -IV) were described previously.[27] The human β-catenin complementary DNA (cDNA) lacking the N-terminal casein kinase I/glycogen synthase kinase 3β (CKI/GSK3β)-phosphorylation sites (β-catenin ΔN134)[11] and the full-length human TCF4 (splice form E) cDNA[28] were subcloned into pCIneo-hemagglutinin (HA) (Promega, Madison, WI). Ran-binding protein 2 (RanBP2) cDNA was subcloned into pcDNA3.1 as described previously.[11] pcDNA3.1-Ubc9 was kindly provided by Dr Van G. Wilson (Texas A&M University System Health Science Center, Dallas, TX). Histone deacetylase 7 (HDAC7) was amplified using a pair of primers, CCACCATGCACAGCCCCGGCGCTGAT and CCTTAGAGATTCATAGGTTCTTCCTCCT, and cloned into pcDNA3.1. A plasmid encoding His-tagged mature SUMO1 (His-SUMO1) was reconstructed from pcDNA3.1-SUMO1 (GG).[11] His-tagged mature SUMO2 (His-SUMO2) was amplified using a pair of primers, CCACCATGCACCATCATCACCACCATGAGACTCCGGCGCTCGCCATGG and TCAACCTCCCGTCTGCTGTTGGAACACATCA, and subcloned into pcDNA3.1. The serially truncated forms of β-catenin cDNA were subcloned into pBIND (Promega). Glutathione *S*-transferase (GST)-PML-IV was constructed by subcloning PML-IV cDNA into pEU-E01-MCS (CellFree Science, Matsuyama, Japan). SUMOylation site-mutated PML-IV was constructed by mutagenesis of GST-PML-IV or Flag-PML-IV using the following primers: K65R-F, CGGTGCCCGAAGCTGCTGCCTTGT; K65R-R, GGCTTCCGCCTGGCATTGCT; K160R-F, CGGCACGAGGCCCGGCCCCTAGCAGA; K160R-R, GAGGAACCACTGGTGTGCCTCGAAGCA; K490R-F, CGGATGGAGTCTGAGGAGGGGAAGGAGGCAA; and K490R-R, GATGACCTTCCTGGGGCACTGGGT. Reporter plasmids encoding p53-responsive firefly luciferase as well as constitutively expressing Renilla luciferase were purchased from SA Biosciences (Frederick, MD).

Silencer negative controls #1 and #2 and silencer small interfering RNA (siRNA) for *CTNNB1* (#42816 and #3000; Ambion, Austin, TX) were used at a final concentration of 20 nmol/L. siRNAs for RanBP2 have been described previously.[11] Transient transfections were performed using the Lipofectamine 2000 and Plus reagents (Invitrogen, Carlsbad, CA) in accordance with the manufacturer's protocol. The total amount of DNA was adjusted by adding relevant empty vectors.

Immunoprecipitation

Cells were lysed in immunoprecipitation buffer (250 mmol/L NaCl, 50 mmol/L Tris-HCl at pH 7.5, 1 mmol/L EDTA, and 0.5% Nonidet P-40 [Fluka, Buchs, Schwitzerland]) supplemented with 1 mmol/L NaF, 10 mmol/L *N*-ethylmaleimide (Sigma-Aldrich), a phosphatase inhibitor cocktail (Sigma-Aldrich), and a protease inhibitor cocktail (Roche, Mannheim, Germany). The lysate was incubated with anti-Flag M2 monoclonal antibody (Sigma-Aldrich), anti-β-catenin monoclonal antibody (clone 14; BD Transduction Laboratories, Palo Alto, CA), anti-TCF4 monoclonal antibody (6H5-3; Upstate, Charlottesville, VA), anti-polyhistidine (clone HIS-1; Sigma-Aldrich), or relevant control immunoglobulin G at 4°C overnight and precipitated with Dynabeads protein G (Dynal Biotech, Oslo, Norway). Immunoprecipitates were washed 5 times with the ice-cold immunoprecipitation buffer and resolved by sodium dodecyl sulfate-polyacrylamide gel electrophoresis (SDS-PAGE).

Immunoblotting

Protein samples were fractionated by SDS-PAGE and blotted onto Immobilon-P membranes (Millipore, Billerica, MA). After incubation with primary antibodies at 4°C overnight, the blots were detected with relevant horseradish peroxidase-conjugated anti-mouse or anti-rabbit immunoglobulin G antibody and ECL Western Blotting Detection Reagents (GE Healthcare, Chalfont St. Giles, United Kingdom). Blot intensity was quantified using a LAS-3000 scanner and Science Lab 2003 software (Fuji Film, Tokyo, Japan).

Anti-β-catenin (clone 14, BD Transduction Laboratories), anti-β-catenin (Cell Signaling Technology, Beverly, MA), anti-TCF4 (6H5-3; Upstate), anti-TCF4 (Santa Cruz Biotechnology, Santa Cruz, CA), anti-GAL4 (RK5C1; Santa Cruz Biotechnology), anti-polyhistidine (clone HIS-1; Sigma-Aldrich), anti-SUMO1 (Biomol Research Laboratory, Plymouth Meeting, PA), anti-SUMO2/3 (Biomol Research Laboratory), anti-β-actin (AC-74; Sigma-Aldrich), anti-p53 (DO-1; Santa Cruz Biotechnology), anti-PML (H-238; Santa Cruz Biotechnology), anti-Ubc9 (Abgent, San Diego, CA), and anti-HDAC7 (XX-7; Santa Cruz Biotechnology) antibodies as well as peroxidase-conjugated anti-Flag (M2; Sigma-Aldrich) antibody were used as the primary antibodies.

Immunofluorescence Microscopy

Cells cultured on glass coverslips (Asahi Technoglass, Tokyo, Japan) were fixed with 4% formaldehyde at room temperature for 10 minutes, permeabilized with 0.1% Triton X-100, and blocked with 10% normal swine serum (Vector Laboratories, Burlingame, CA). Twelve specimens of sporadic colorectal cancer were selected from the pathology archive panel of the National Cancer Center Hospital (Tokyo, Japan). The specimens were incubated with primary antibodies at 4°C overnight and subsequently with Alexa Fluor-conjugated secondary antibodies (Invitrogen). Images were taken on a Zeiss Axioplan 2 microscope (Carl Zeiss, Gottingen, Germany). Primary antibodies used in this study were anti-Flag (M2), anti-HA (Bethyl Laboratories, Montgomery, TX), anti-PML-IV[29] (kindly provided by Dr Hugues de Thé and Dr Morgane Le Bras, INSERM/Centre National de la Recherche Scientifique [CNRS], Paris, France), and anti-β-catenin (clone 14) monoclonal antibodies. The protocol was reviewed and approved by the institutional ethics board of the National Cancer Center (Tokyo, Japan).

In Vitro Binding Assay

GST-fused PML-IV and the SUMOylation site-mutated recombinant proteins were synthesized using the ENDEXT Wheatgerm Expression Kit (CellFree Sciences, Matsuyama, Japan), incubated with Glutathione Sepharose 4B (GE Healthcare), washed with phosphate-buffered saline, and then eluted by adding elution buffer (50 mmol/L Tris-HCl, 10 mmol/L reduced glutathione, pH 8.0). Recombinant GST and GST-β-catenin fusion proteins were purchased from Abcam (Cambridge, England). Recombinant GST-RanBP2ΔFG (amino acids 2553–2838)[11] and His-HDAC7 proteins were purchased from Biomol Research Laboratory and Millipore, respectively.

Flag-tagged PML-IV protein was purified with anti-Flag M2 affinity gel (Sigma-Aldrich), incubated with 1 μg of GST-RanBP2ΔFG or His-HDAC7 and 1 μg of GST or GST-β-catenin, washed 5 times with phosphate-buffered saline, and then resolved by SDS-PAGE.

In Vitro SUMOylation Assay

In vitro SUMOylation was performed in a total volume of 40 μL in 40 mmol/L Tris-HCl (pH 7.5) with 0.75 mmol/L dithiothreitol at 37°C for 10 minutes (SUMO1) or 1 hour (SUMO2), terminated by addition of SDS sample buffer, and analyzed by SDS-PAGE and immunoblotting.

Results

Interaction of PML-IV With β-Catenin and TCF4

Using a comprehensive shotgun mass spectrometry approach, we had previously identified PML as 1 of 70 proteins commonly coimmunoprecipitated with anti-TCF4 antibody from 2 colorectal cancer cell lines, DLD-1 and HCT116,[11] although its biological significance had remained unexplored. The *PML* gene generates several alternatively spliced transcripts with different C-termini. Each PML isoform has different protein partners and mediates distinct cellular functions.[30] To verify the protein interaction identified by mass spectrometry and determine which PML isoform forms a complex with TCF4 and β-catenin, FLAG-tagged PML isoforms (I to V) were cotransfected with TCF4 and β-cateninΔN134 into HEK293 cells. Cell lysates were immunoprecipitated with anti-FLAG, anti-TCF4, or anti-β-catenin antibody and blotted with anti-FLAG, anti-β-catenin (β-cat), and anti-TCF4 antibodies (Figure 1*A*). We found that only PML-IV was coimmunoprecipitated with TCF4 and β-catenin, whereas the other isoforms showed no or little interaction with them. These results indicated that PML-IV is the PML isoform that interacts specifically with the TCF4 and β-catenin protein complex. We examined serial deletion mutants of β-catenin (Figure 1*B*) for binding with GST-PML-IV and found that a region containing armadillo repeats was responsible for the interaction with PML-IV (Figure 1*C*).

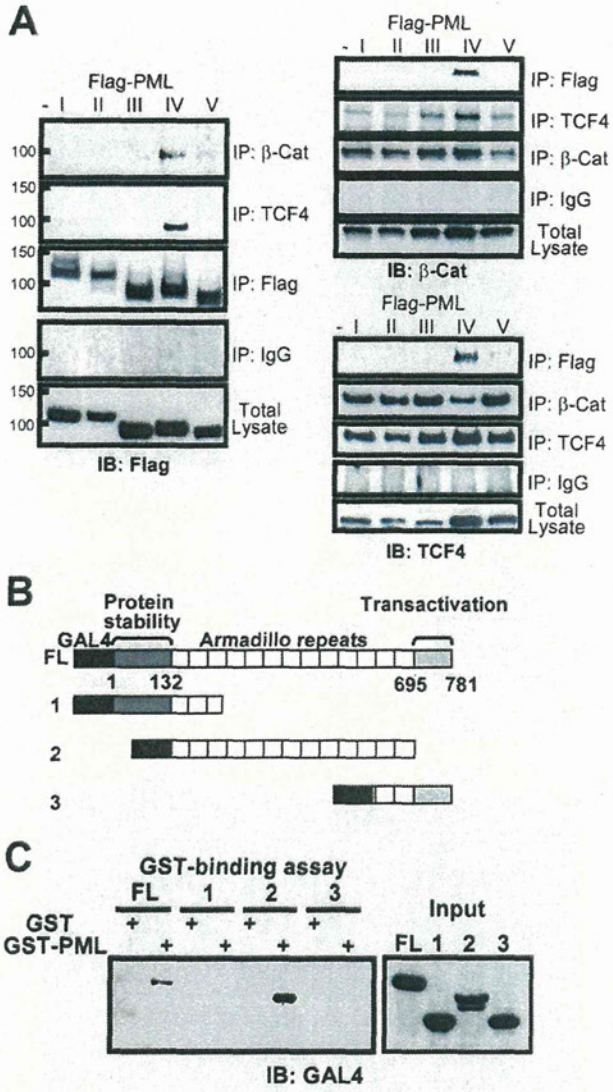

Figure 1. Interaction of PML-IV with β-catenin. (*A*) HEK293 cells were transfected with Flag-PML-I to -V, HA-β-cateninΔN134, and TCF4. The cell lysate was immunoprecipitated with anti-Flag, anti–β-catenin (β-cat), or anti-TCF4 antibody or normal mouse immunoglobulin (Ig) G. Total lysates and immunoprecipitates (IP) were immunoblotted (IB) with the indicated antibodies. (*B*) Schematic representation of the full-length (FL) and serially truncated forms of β-catenin constructs. (*C*) The β-catenin constructs were transfected into HEK293 cells. Cell lysates were incubated with GST (negative control) or GST-PML-IV, precipitated with Glutathione Sepharose 4B, and then resolved by SDS-PAGE. Total lysates (Input) and immunoprecipitates were immunoblotted with anti-GAL4 antibody.

β-Catenin Inhibits NB Formation of PML-IV

To investigate the effect of β-catenin on PML-NB formation, HeLa cells, which carry the wild-type *APC* and *CTNNB1* genes, were transfected with the Flag-tagged PML-IV (Flag-PML-IV) and HA-tagged β-cateninΔN134 constructs, and the subcellular localization of their expressed protein was examined by immunofluorescence microscopy. In HeLa cells expressing a low amount of β-catenin protein, the fine speckles of PML-IV protein were distributed uniformly within nuclei and showed the typical punctate pattern, whereas in cells expressing a high amount of β-catenin (indicated by *arrows* in Figure 2*A*) PML-IV was coarsely aggregated and distributed irregularly. These findings indicated that the presence of excess

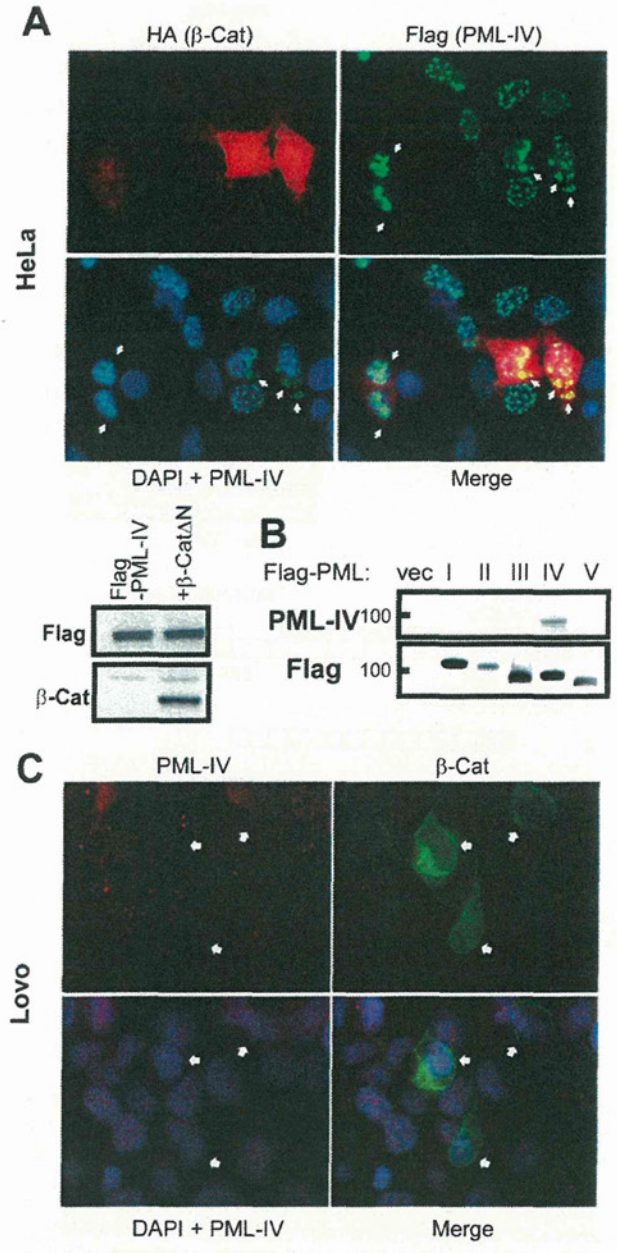

Figure 2. β-Catenin disrupts the compartmentalization of PML-IV. (*A*) HeLa cells were cotransfected with HA-β-cateninΔN134 and Flag-PML-IV and stained with anti-HA (*red*) and Flag (*green*) antibodies. Cell nuclei were visualized using 4′,6-diamidino-2-phenylindole (DAPI) (*blue*). *White arrows* indicate cells with overexpression of β-catenin and abnormal compartmentalization of PML-IV. (*B*) Control pLNCX vector (vec) or Flag-PML-I to -V was transfected into HeLa cells, and the cell lysates were immunoblotted with anti–PML-IV or anti-Flag antibody. (*C*) Lovo cells were transfected with siRNA against β-catenin. Immunofluorescence staining was performed with anti–PML-IV (*red*) and anti–β-catenin (*green*) antibodies. Cell nuclei are visualized using DAPI (*blue*).

β-catenin protein interfered with the normal compartmentalization of PML-IV.

We next examined the effect of β-catenin knockdown on PML-NB formation. Colorectal cancer cells were transfected with siRNAs against β-catenin, and the distribution of endogenous PML-IV was evaluated by immunofluorescence microscopy with isoform-specific anti-PML-IV antibody,[29] the specificity of which was confirmed by immunoblotting (Figure 2*B*). PML-IV speckles were restored by knocking down β-catenin, whereas little or broad PML-IV staining was observed in colorectal cancer cells maintaining β-catenin expression (Figure 2*C*).

In the clinical specimens from patients with colorectal cancer, normal intestinal epithelial cells without nuclear β-catenin accumulation showed the regular nuclear speckles of PML-IV, whereas no or few speckles were observed in colorectal cancer cells with nuclear β-catenin accumulation (Figure 3). These results were consistent with those of the aforementioned transfection experiments.

β-Catenin Inhibits SUMOylation of PML-IV

SUMOylation of PML is essential for the proper assembly of PML-NB. In fact, SUMOylation-deficient PML shows aberrant nuclear localization.[31,32] To test whether the aberrant PML-IV compartmentalization induced by β-catenin is due to deficient SUMOylation of PML-IV, HeLa cells were transfected with HA-β-cateninΔN134 along with Flag-tagged PML-IV and His-tagged SUMO1 (Figure 4*A*, *left*) or SUMO2 (Figure 4*A*, *right*). Immunoprecipitation and immunoblot analysis showed significantly reduced SUMOylation of PML-IV in cells cotransfected with HA-β-cateninΔN134 (Figure 4*A*). However, β-catenin did not affect the SUMOylation of PML-I or PML-III (Figure 4*B*), suggesting that the overexpression of β-catenin specifically inhibits the SUMOylation of PML-IV.

Knockdown of β-catenin in colorectal cancer DLD1 cells by siRNA (si-βc1 and si-βc2) increased the amount of PML-IV protein modified by SUMO1 (Figure 5*A*) and SUMO2 (Figure 5*B*). Similar results were obtained in 2 other colorectal cancer cell lines, Lovo and SW48 (data not shown). These data support the notion that accumulation of β-catenin interferes with the SUMOylation of PML-IV.

β-Catenin Inhibits RanBP2-Mediated SUMOylation of PML-IV

Small ubiquitin-like modifier (SUMO) proteins, a superfamily of ubiquitin-like proteins, are covalently conjugated to their substrate proteins through a cascade mediated by SUMO E1-activating, E2-conjugating, and E3-ligating enzymes. Because β-catenin did not affect the SUMOylation of PML-IV in the presence of SUMO-activating enzyme Aos1/Uba2 (E1) and conjugating enzyme Ubc9 (E2) (Figure 5*C* and *D*), we tested the effects of β-catenin on the E3-ligating reaction of PML-IV.

HDAC7[33] and RanBP2[34,35] have been shown to have the E3 SUMO ligase activity for PML and to be essential for PML-NB formation. The in vitro binding assay showed that β-catenin inhibited the physical interaction between PML-IV and RanBP2 but not that between PML-IV and HDAC7 (Figure 6*A*). We had previously identified RanBP2 as a component of the TCF4 and β-catenin complex.[11] The SUMOylation of PML-IV by RanBP2 was inhibited in the presence of β-catenin (Figure 6*B*). When RanBP2 was

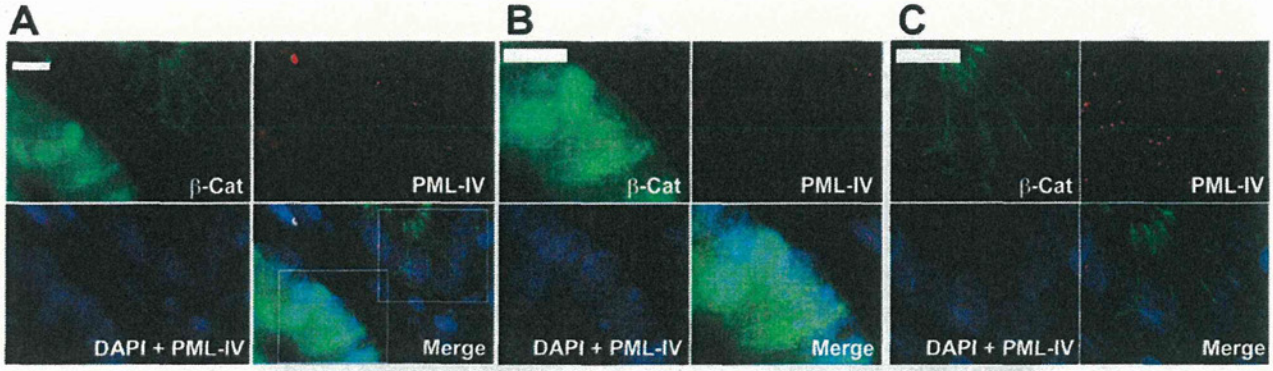

Figure 3. Absence of PML-IV speckles in colorectal cancer. Clinical specimens from patients with colorectal cancer were subjected to immunofluorescence staining with anti–PML-IV (*red*) and anti–β-catenin (*green*) antibodies. Cell nuclei are visualized using DAPI (*blue*). *Scale bar* = 10 μm. Boxed regions in *A* were enlarged and are shown in *B* and *C*.

transfected into HeLa cells, the SUMOylation of PML-IV was increased, and this increase was suppressed by coexpression of β-cateninΔN134 (Figure 6*C*). These results revealed that β-catenin prevents RanBP2-mediated enhancement of PML-IV SUMOylation by sequestering PML-IV from RanBP2.

SUMOylation of the Lysine 490 Residue of PML-IV by RanBP2

PML has several potential SUMOylation sites, each of which is considered to mediate a different aspect of the compartmentalization and stabilization of PML.[36,37] To determine the SUMOylation site of PML-IV by RanBP2, we produced PML-IV constructs mutated at the 65 (K65R), 160 (K160R), and 490 (K490R) lysine residues and assessed their SUMOylation by RanBP2 (Figure 6*D*). We found that the K65R and K160R constructs were SUMOylated by RanBP2, whereas the K490R construct was not, indicating that the lysine 490 residue of PML-IV is SUMOylated by RanBP2. To examine whether the SUMOylation at lysine 490 is essential for the proper assembly of PML-NB, HeLa cells were transfected with the Flag-PML-IV K490R, and its subcellular localization was examined by immunofluorescence microscopy.

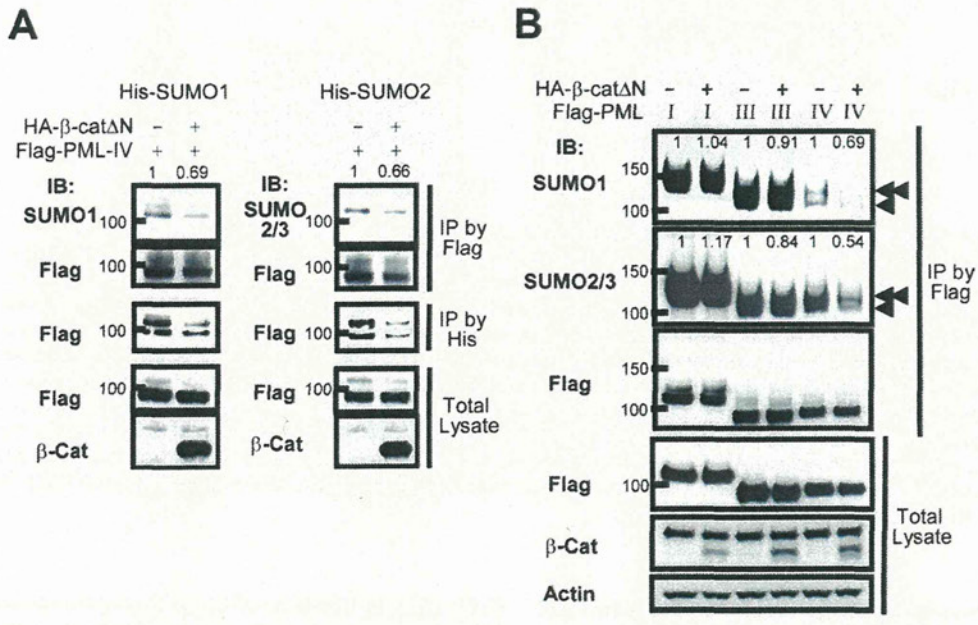

Figure 4. β-Catenin inhibits the SUMOylation of PML-IV. (*A*) Flag-PML-IV, HA-β-cateninΔN134 (HA-β-catΔN) (+) or pCIneo-HA (−), and His-SUMO1 (*left*) or His-SUMO2 (*right*) were transfected into HeLa cells as indicated. Total cell lysates were immunoprecipitated with anti-Flag or anti-His antibody. Total lysates and immunoprecipitates (IP) were immunoblotted (IB) with the indicated antibodies. Values above the blots indicate the relative amounts of SUMOylated Flag-PML-IV (SUMO1 or SUMO2/3) (normalized to immunoprecipitated Flag-PML-IV [Flag]). The values for HA-β-catΔN (−) were set at 1. (*B*) Flag-PML-I, -III, or -IV, HA-β-cateninΔN134 (HA-β-catΔN) (+) or pCIneo-HA (−), and His-SUMO1 were transfected into HeLa cells in the indicated combinations. Immunoprecipitation and immunoblotting were performed with the indicated antibodies. *Arrowheads* indicate mono-SUMOylated (*single arrowheads*) and poly-SUMOylated (*double arrowheads*) PLM-IV. Values above the blots indicate the relative amounts of SUMOylated Flag-PML-IV (SUMO1 or SUMO2/3) (normalized to immunoprecipitated Flag-PML-IV [Flag]). The values for HA-β-catΔN (−) were set at 1.

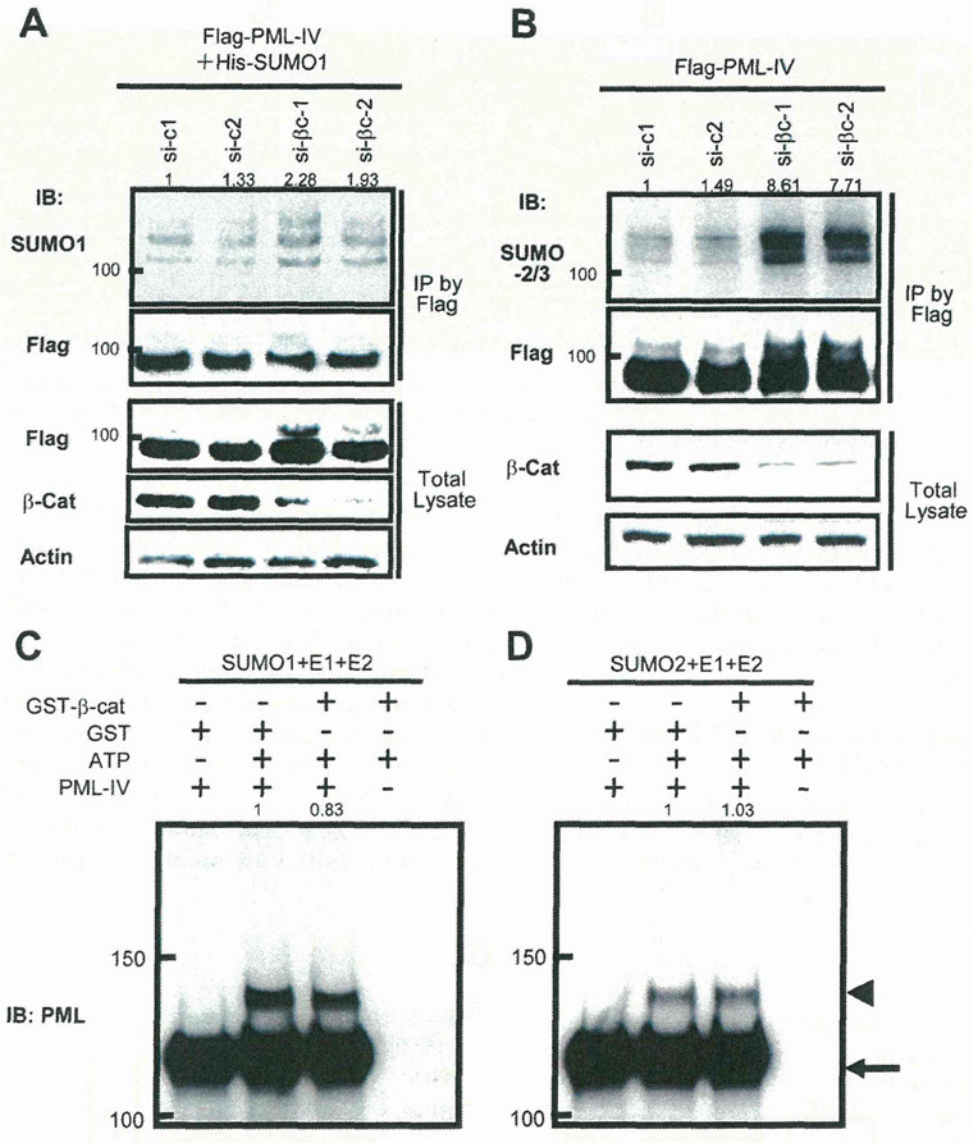

Figure 5. Knockdown of β-catenin restores the SUMOylation of PML-IV. (*A*) Flag-PML-IV, His-SUMO1, and control RNA (si-c1 or si-c2) or siRNA against β-catenin (si-βc1 or si-βc2) were transfected into DLD1 cells, and the cell lysates were immunoprecipitated with anti-Flag antibody. Total lysates and immunoprecipitates (IP) were immunoblotted (IB) with the indicated antibodies. Values above the blots indicate the amounts of SUMOylated Flag-PML-IV (SUMO1) relative to si-c1 (control siRNA) (normalized to immunoprecipitated Flag-PML-IV [Flag]). (*B*) Flag-PML-IV and control RNA (si-c1 or si-c2) or siRNA against β-catenin (si-βc1 or si-βc2) were transfected into DLD-1 cells, and the cell lysate was immunoprecipitated with anti-Flag antibody. Total lysates and immunoprecipitates were immunoblotted with the indicated antibodies. Values above the blots indicate the amounts of SUMOylated Flag-PML-IV (SUMO2/3) relative to si-c1 (control siRNA) (normalized to immunoprecipitated Flag-PML-IV [Flag]). (*C* and *D*) Purified Flag-PML-IV protein was incubated with GST (1 μg) or GST–β-catenin (β-cat) (1 μg), SUMO-activating enzyme Aos1/Uba2 (E1) (0.3 μg), conjugating enzyme Ubc9 (E2) (0.2 μg), and (*C*) His-SUMO1 (3 μg) or (*D*) His-SUMO2 (3 μg) at 37°C for 1 hour in the presence or absence of 4 mmol/L adenosine triphosphate (ATP), and SUMOylated PML-IV proteins were detected as slowly migrating bands (indicated by an *arrowhead*) by immunoblotting with anti-PML antibody. Values above the blots indicate the relative amounts of SUMOylated Flag-PML-IV (*arrowhead*) (normalized to immunoprecipitated Flag-PML-IV [*arrow*]).

PML-IV K490R was coarsely aggregated and distributed irregularly (Figure 6*E*).

β-Catenin Abrogates the Transactivation of TP53 by PML-IV

Finally we examined whether the abrogation of PML-IV compartmentalization by β-catenin leads to the suppression of PML function. p53 activity is regulated by PML, and stabilization of the p53 protein mediates in part the tumor-suppressor function of PML.[38-40] Consistently, the luciferase activity driven by the p53-responsive promoter was enhanced 2-fold by transfection with PML-IV, and the enhancement was suppressed by increasing the amount of coexpressed β-catenin (Figure 7*A*). Overexpression of PML-IV induced the accumulation of p53 protein, and this was suppressed by increasing the amount of

BASIC AND TRANSLATIONAL AT

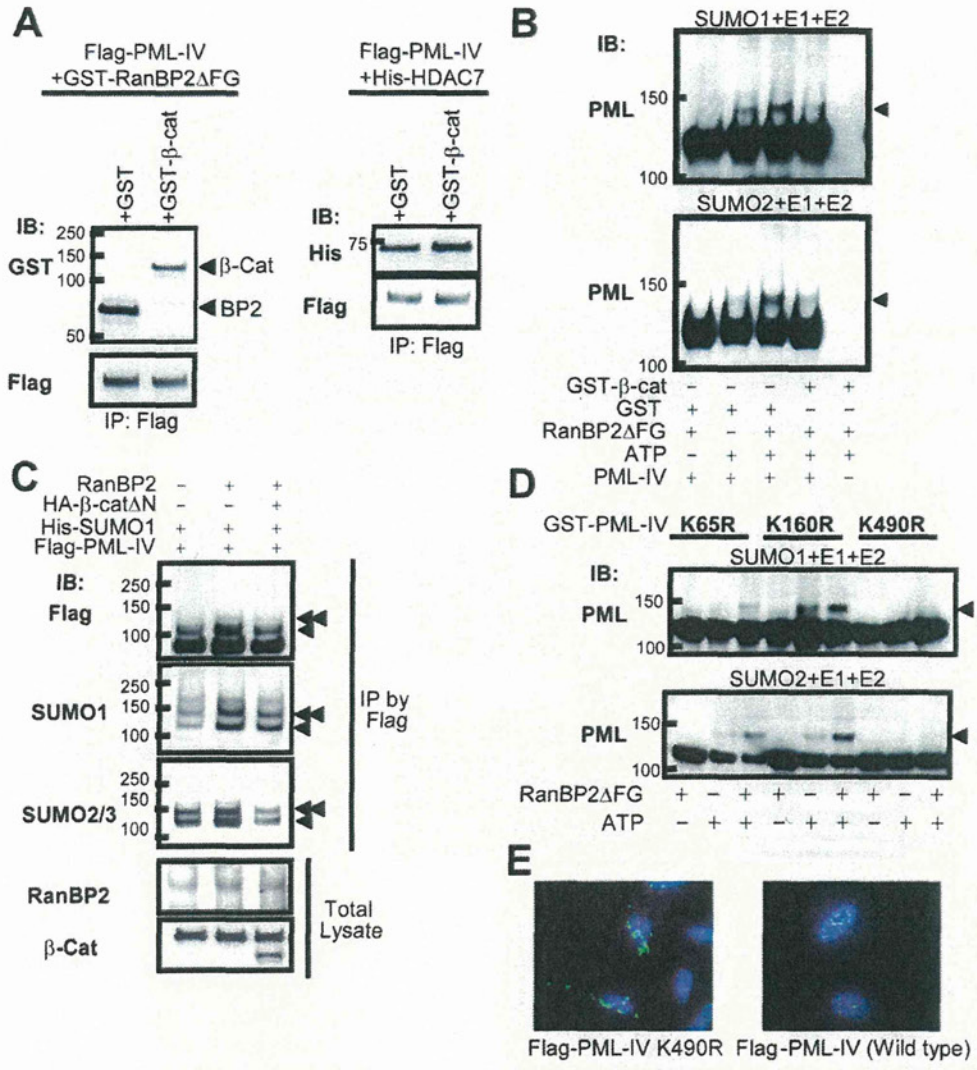

Figure 6. β-Catenin inhibits RanBP2-mediated SUMOylation of PML-IV. (*A*) Purified Flag-PML-IV protein and GST-RanBP2ΔFG or His-HDAC7 were incubated in the presence of GST or GST-β-catenin protein, immunoprecipitated (IP) with anti-Flag antibody, and immunoblotted (IB) with anti-GST, anti-His, or anti-Flag antibody. (*B*) Recombinant PML-IV, RanBP2dFG (25 ng), and GST or GST-β-catenin (1 μg) were incubated with E1 (0.3 μg), E2 (0.2 μg), SUMO1 (3 μg) or SUMO2 (3 μg), and 4 mmol/L adenosine triphosphate (ATP) as indicated. (*C*) Flag-PML-IV, His-SUMO1, HA-β-cateninΔN134 (HA-β-catΔN), and RanBP2 were transfected into HeLa cells in the indicated combinations. Immunoprecipitation and immunoblotting were performed with the indicated antibodies. (*D*) Recombinant GST-PML-IV protein with mutation in the lysine 65, 160, or 490 residue and RanBP2ΔFG (25 ng) were incubated with E1 (0.3 μg), E2 (0.2 μg), SUMO1 (3 μg) or SUMO2 (3 μg), and 4 mmol/L ATP as indicated. SUMOylated PML-IV (indicated by *arrowheads*) was detected by SDS-PAGE and immunoblotting with anti-PML antibody. (*E*) HeLa cells were transfected with Flag-PML-IV K490R (*left*) or with Flag-PML-IV (wild type) and stained with anti-Flag (*green*) antibody. Nuclei were visualized with DAPI staining (*blue*).

coexpressed β-catenin (Figure 7*B*). Furthermore, p53 accumulation by PML-IV was enhanced by RanBP2, and the enhancement was abrogated by the coexpression of β-catenin (Figure 7*C*). Knockdown of RanBP2 suppressed p53-responsive promoter activity (Figure 7*D*), and the PML mutants K490R and K160R failed to fully activate the p53-responsive promoter (Figure 7*E*). SUMOylation of the lysine 160 residue of PML-IV by SUMO3 has also been shown to be essential for PML-NB formation.[41] Enhancement of p53-responsive promoter activity by Ubc9 or HDAC7 was insensitive to β-catenin (Figure 7*F*). All these results indicate that the lysine 490 residue of PML-IV is the likely RanBP2 target site and that β-catenin inhibits the SUMOylation via competitive binding with RanBP2.

Discussion

Aberrant activation of Wnt signaling and subsequent accumulation of β-catenin has been considered a major force driving development of colorectal cancer, but β-catenin is a multifunctional protein, and the entire process of carcinogenesis mediated by its accumulation has not been fully explained. In this study, we revealed a

BASIC AND TRANSLATIONAL AT

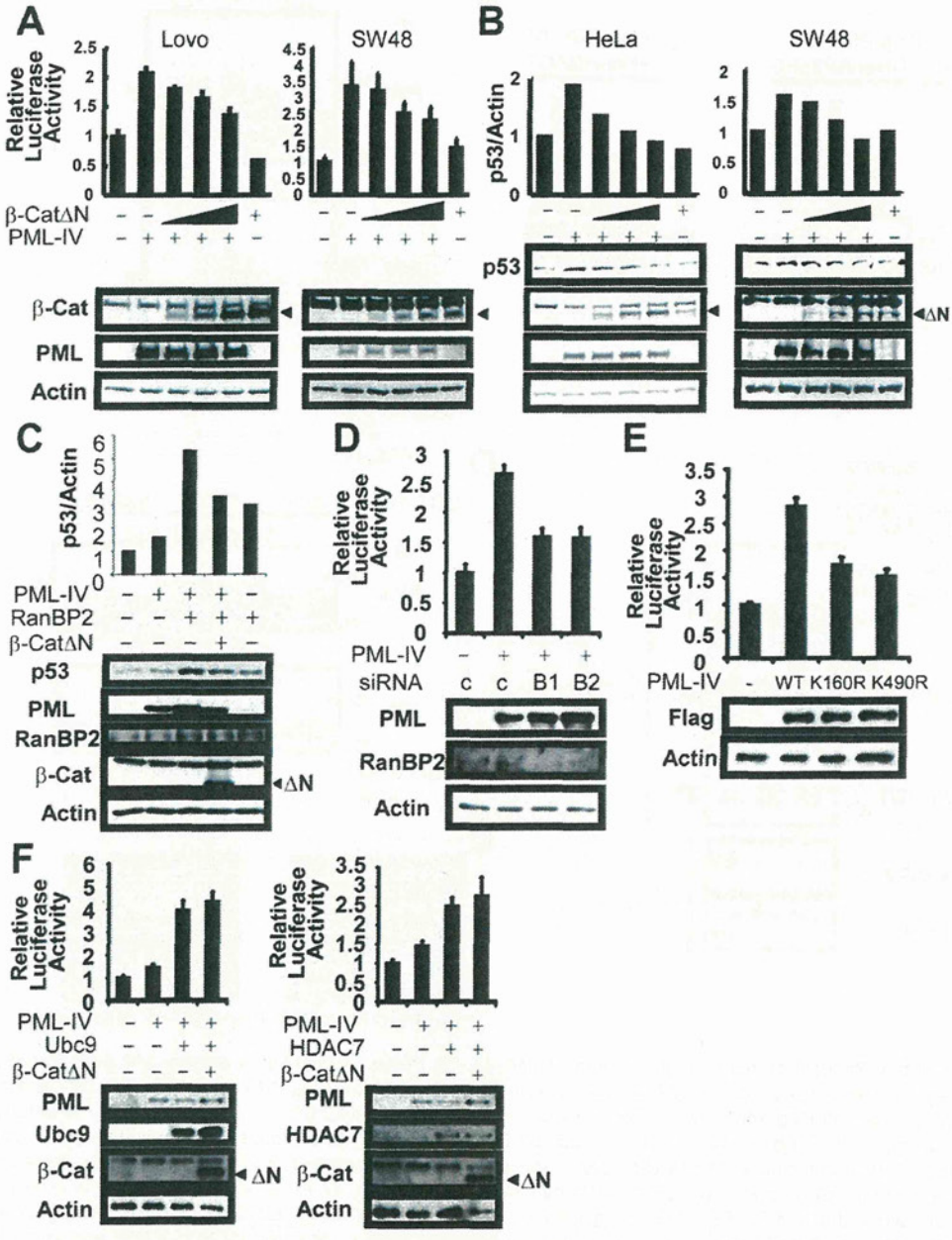

Figure 7. β-Catenin interferes with p53 activation by PML-IV. (*A*) Lovo or SW48 cells were transfected in triplicate with a p53-responsive firefly luciferase construct, a constitutively expressed Renilla luciferase construct, Flag-PML-IV, and β-cateninΔN134 (β-catΔN) or their relevant empty vectors as indicated. Forty-eight hours after transfection, luciferase activity was measured using Renilla luciferase activity as the internal control. *Bars* represent SD. (*B*) Flag-PML-IV and β-cateninΔN134 (β-catΔN) were transfected into HeLa or SW48 cells as indicated. Twenty-four hours later, the cells were treated with mitomycin C (10 μmol/L) for 3 hours and harvested with SDS sample buffer. Lysates were immunoblotted with the indicated antibodies. The intensity of the blots was quantified by densitometry, and the expression level of p53 protein relative to β-actin (internal control) was calculated. (*C*) Flag-PML-IV, RanBP2, and β-cateninΔN134 (β-catΔN) were transfected into HeLa cells as indicated. The relative expression level of p53 protein was determined as described in *B*. (*D*) Lovo cells were transfected in triplicate with a p53-responsive firefly luciferase construct, a Renilla luciferase construct, Flag-PML-IV, and siRNA (C, control; B1 and B2, siRNA for RanBP2[11]) as indicated. Luciferase activity was measured as described in *A*. (*E*) Lovo cells were transfected in triplicate with a p53-responsive firefly luciferase construct, a constitutively expressed Renilla luciferase construct, and Flag-PML-IV (WT, K160R, or K490R) as indicated, and luciferase activity was measured as described in *A*. (*F*) Lovo cells were transfected in triplicate with a p53-responsive firefly luciferase construct, a constitutively expressed Renilla luciferase construct, Flag-PML-IV, Ubc9, HDAC7, and β-cateninΔN134 (β-catΔN) as indicated, and luciferase activity was measured as described in *A*.

novel posttranslational mechanism by which β-catenin abrogated PML tumor suppressor function. β-catenin forms a complex specifically with PML-IV (Figure 1) and sequesters PML-IV from RanBP2 (Figure 6*A*). RanBP2 has been shown to be an E3 ligase for PML-IV,[34,35] and this sequestering inhibited the SUMOylation of PML-IV (Figure 6*B* and *C*). SUMOylation of PML is essential for the recruitment of several PML-binding proteins and

proper assembly of PML-NB.[32,37,42] The accumulation of β-catenin was closely associated with aberrant PML-NB formation in clinical samples (Figure 3). We conclude that β-catenin disrupts PML-NB formation by inhibiting the SUMOylation of PML-IV by RanBP2. However, the possibility that RanBP2 regulates other scaffold or associated proteins that aid the recruitment of PML-IV could not be fully excluded.

The integrity of PML-NB is essential for proper gene transcription. We observed that β-catenin inhibited the PML-mediated enhancement of promoter-specific transcriptional activity of p53 tumor suppressor protein (Figure 7). PML interacts with p53 protein and recruits it into PML-NB.[38] The disruption of PML-NB formation by β-catenin thus seems to inhibit the recruitment of p53 and its tumor-suppressor function.

Reduced expression of PML protein is not limited to colorectal cancer but has also been reported in various human solid tumors, including cancers of the prostate, breast, lung, and brain,[26] where this loss of expression is associated with aggressive tumor behavior in some cases. However, expression of the *PML* gene was well maintained, and its mutation was rare in solid tumors, indicating the contribution of certain posttranslational mechanisms to the reduction of PML protein expression. A recent study has shown that SUMOylation of PML leads to its degradation through recognition by the E3 ubiquitin ligase RNF4/SNURF, a protein containing 4 SUMO interaction motifs.[43] On the other hand, it has also been shown that SUMOylation inhibits the degradation of PML by Pin1, peptidyl-prolyl cis-trans isomerase, which binds to phosphorylated PML and promotes a conformational change triggering its degradation.[44] This apparent contradiction could be explained by assuming that each SUMOylation site in PML mediates a different function.[36] SUMOylation of the lysine 160 residue promotes PML degradation by RNF4/SNURF, whereas SUMOylation of lysine 490 inhibits PML degradation.[43] RanBP2 SUMOylates the lysine 490 residue, but not the lysine 160 residue, of PML-IV (Figure 6*D*). β-Catenin is considered to promote the dysfunction of PML through inhibition of residue-specific SUMOylation.

The Wnt signaling pathway plays important roles in the maintenance of intestinal epithelial stem cell reservoirs.[45] Constitutive activation of the pathway has been implicated in the maintenance of the undifferentiated status and self-renewal of colorectal cancer cells. Recently, PML was also reported to be essential for the maintenance of hematopoietic stem and quiescent leukemia-initiating cells.[46] The inorganic arsenite arsenic trioxide has been shown to target PML for degradation[47] and to eradicate quiescent leukemia-initiating chronic myeloid leukemia cells.[46] In the present study, although we focused mainly on the inhibition of PML SUMOylation by β-catenin, the interaction between the 2 proteins may have different functional aspects that are essential for the regulation of stem cell phenotype. It will be necessary to further clarify the entire signaling pathway mediated by these proteins.

References

1. Kinzler KW, Vogelstein B. Lessons from hereditary colorectal cancer. Cell 1996;87:159–170.
2. Morin PJ, Sparks AB, Korinek V, et al. Activation of beta-catenin-Tcf signaling in colon cancer by mutations in beta-catenin or APC. Science 1997;275:1787–1790.
3. Sparks AB, Morin PJ, Vogelstein B, et al. Mutational analysis of the APC/beta-catenin/Tcf pathway in colorectal cancer. Cancer Res 1998;58:1130–1134.
4. Barker N, Morin PJ, Clevers H. The yin-yang of TCF/beta-catenin signaling. Adv Cancer Res 2000;77:1–24.
5. Shitashige M, Hirohashi S, Yamada T. Wnt signaling inside the nucleus. Cancer Sci 2008;99:631–637.
6. Idogawa M, Yamada T, Honda K, et al. Poly(ADP-ribose) polymerase-1 is a component of the oncogenic T-cell factor-4/beta-catenin complex. Gastroenterology 2005;128:1919–1936.
7. Idogawa M, Masutani M, Shitashige M, et al. Ku70 and poly(ADP-ribose) polymerase-1 competitively regulate beta-catenin and T-cell factor-4-mediated gene transactivation: possible linkage of DNA damage recognition and Wnt signaling. Cancer Res 2007;67:911–918.
8. Sato S, Idogawa M, Honda K, et al. beta-catenin interacts with the FUS proto-oncogene product and regulates pre-mRNA splicing. Gastroenterology 2005;129:1225–1236.
9. Shitashige M, Naishiro Y, Idogawa M, et al. Involvement of splicing factor-1 in beta-catenin/T-cell factor-4-mediated gene transactivation and pre-mRNA splicing. Gastroenterology 2007;132:1039–1054.
10. Hayashida Y, Honda K, Idogawa M, et al. E-cadherin regulates the association between beta-catenin and actinin-4. Cancer Res 2005;65:8836–8845.
11. Shitashige M, Satow R, Honda K, et al. Regulation of Wnt signaling by the nuclear pore complex. Gastroenterology 2008;134:1961–1971, 1971 e1–4.
12. Kakizuka A, Miller WH Jr, Umesono K, et al. Chromosomal translocation t(15;17) in human acute promyelocytic leukemia fuses RAR alpha with a novel putative transcription factor, PML. Cell 1991;66:663–674.
13. de The H, Lavau C, Marchio A, et al. The PML-RAR alpha fusion mRNA generated by the t(15;17) translocation in acute promyelocytic leukemia encodes a functionally altered RAR. Cell 1991;66:675–684.
14. Wang ZG, Delva L, Gaboli M, et al. Role of PML in cell growth and the retinoic acid pathway. Science 1998;279:1547–1551.
15. Piazza F, Gurrieri C, Pandolfi PP. The theory of APL. Oncogene 2001;20:7216–7222.
16. Melnick A, Licht JD. Deconstructing a disease: RARalpha, its fusion partners, and their roles in the pathogenesis of acute promyelocytic leukemia. Blood 1999;93:3167–3215.
17. Salomoni P, Pandolfi PP. The role of PML in tumor suppression. Cell 2002;108:165–170.
18. Bernardi R, Papa A, Pandolfi PP. Regulation of apoptosis by PML and the PML-NBs. Oncogene 2008;27:6299–6312.
19. Salomoni P, Ferguson BJ, Wyllie AH, et al. New insights into the role of PML in tumour suppression. Cell Res 2008;18:622–640.
20. Labbaye C, Valtieri M, Grignani F, et al. Expression and role of PML gene in normal adult hematopoiesis: functional interaction between PML and Rb proteins in erythropoiesis. Oncogene 1999;18:3529–3540.
21. Guo A, Salomoni P, Luo J, et al. The function of PML in p53-dependent apoptosis. Nat Cell Biol 2000;2:730–736.
22. Bernardi R, Guernah I, Jin D, et al. PML inhibits HIF-1alpha translation and neoangiogenesis through repression of mTOR. Nature 2006;442:779–785.
23. Wang ZG, Ruggero D, Ronchetti S, et al. PML is essential for multiple apoptotic pathways. Nat Genet 1998;20:266–272.
24. Rego EM, Pandolfi PP. Analysis of the molecular genetics of acute promyelocytic leukemia in mouse models. Semin Hematol 2001;38:54–70.

25. Cabrera CM, Jimenez P, Concha A, et al. Promyelocytic leukemia (PML) nuclear bodies are disorganized in colorectal tumors with total loss of major histocompatibility complex class I expression and LMP7 downregulation. Tissue Antigens 2004;63:446–452.
26. Gurrieri C, Capodieci P, Bernardi R, et al. Loss of the tumor suppressor PML in human cancers of multiple histologic origins. J Natl Cancer Inst 2004;96:269–279.
27. Nguyen LA, Pandolfi PP, Aikawa Y, et al. Physical and functional link of the leukemia-associated factors AML1 and PML. Blood 2005;105:292–300.
28. Shitashige M, Satow R, Jigami T, et al. Traf2- and Nck-interacting kinase is essential for Wnt signaling and colorectal cancer growth. Cancer Res 2010;70:5024–5033.
29. Condemine W, Takahashi Y, Zhu J, et al. Characterization of endogenous human promyelocytic leukemia isoforms. Cancer Res 2006;66:6192–6198.
30. Jensen K, Shiels C, Freemont PS. PML protein isoforms and the RBCC/TRIM motif. Oncogene 2001;20:7223–7233.
31. Duprez E, Saurin AJ, Desterro JM, et al. SUMO-1 modification of the acute promyelocytic leukaemia protein PML: implications for nuclear localisation. J Cell Sci 1999;112:381–393.
32. Shen TH, Lin HK, Scaglioni PP, et al. The mechanisms of PML-nuclear body formation. Mol Cell 2006;24:331–339.
33. Gao C, Ho CC, Reineke E, et al. Histone deacetylase 7 promotes PML sumoylation and is essential for PML nuclear body formation. Mol Cell Biol 2008;28:5658–5667.
34. Tatham MH, Kim S, Jaffray E, et al. Unique binding interactions among Ubc9, SUMO and RanBP2 reveal a mechanism for SUMO paralog selection. Nat Struct Mol Biol 2005;12:67–74.
35. Saitoh N, Uchimura Y, Tachibana T, et al. In situ SUMOylation analysis reveals a modulatory role of RanBP2 in the nuclear rim and PML bodies. Exp Cell Res 2006;312:1418–1430.
36. Petrie K, Zelent A. Marked for death. Nat Cell Biol 2008;10:507–509.
37. Zhong S, Muller S, Ronchetti S, et al. Role of SUMO-1-modified PML in nuclear body formation. Blood 2000;95:2748–2752.
38. Fogal V, Gostissa M, Sandy P, et al. Regulation of p53 activity in nuclear bodies by a specific PML isoform. EMBO J 2000;19:6185–6195.
39. Zhu H, Wu L, Maki CG. MDM2 and promyelocytic leukemia antagonize each other through their direct interaction with p53. J Biol Chem 2003;278:49286–49292.
40. Bernardi R, Scaglioni PP, Bergmann S, et al. PML regulates p53 stability by sequestering Mdm2 to the nucleolus. Nat Cell Biol 2004;6:665–672.
41. Fu C, Ahmed K, Ding H, et al. Stabilization of PML nuclear localization by conjugation and oligomerization of SUMO-3. Oncogene 2005;24:5401–5413.
42. Ishov AM, Sotnikov AG, Negorev D, et al. PML is critical for ND10 formation and recruits the PML-interacting protein daxx to this nuclear structure when modified by SUMO-1. J Cell Biol 1999;147:221–234.
43. Lallemand-Breitenbach V, Jeanne M, Benhenda S, et al. Arsenic degrades PML or PML-RARalpha through a SUMO-triggered RNF4/ubiquitin-mediated pathway. Nat Cell Biol 2008;10:547–555.
44. Reineke EL, Lam M, Liu Q, et al. Degradation of the tumor suppressor PML by Pin1 contributes to the cancer phenotype of breast cancer MDA-MB-231 cells. Mol Cell Biol 2008;28:997–1006.
45. Korinek V, Barker N, Moerer P, et al. Depletion of epithelial stem-cell compartments in the small intestine of mice lacking Tcf-4. Nat Genet 1998;19:379–383.
46. Ito K, Bernardi R, Morotti A, et al. PML targeting eradicates quiescent leukaemia-initiating cells. Nature 2008;453:1072–1078.
47. Lallemand-Breitenbach V, Zhu J, Puvion F, et al. Role of promyelocytic leukemia (PML) sumolation in nuclear body formation, 11S proteasome recruitment, and As2O3-induced PML or PML/retinoic acid receptor alpha degradation. J Exp Med 2001;193:1361–1371.

Received April 7, 2011. Accepted November 25, 2011.

Reprint requests

Address requests for reprints to: Tesshi Yamada, MD, PhD, Division of Chemotherapy and Clinical Research, National Cancer Center Research Institute, 5-1-1 Tsukiji, Chuo-ku, Tokyo 104-0045, Japan. e-mail: tyamada@ncc.go.jp; fax: (81)3-3547-6045.

Acknowledgments

The authors thank Drs de Thé and Le Bras for provision of the anti-PML-IV antibody and Dr Wilson for providing pcDNA3.1-human Ubc9.

Conflicts of interest

The authors disclose no conflicts.

Funding

Supported by the Program for Promotion of Fundamental Studies in Health Sciences conducted by the National Institute of Biomedical Innovation of Japan and the Third-Term Comprehensive Control Research for Cancer and Research on Biological Markers for New Drug Development conducted by the Ministry of Health, Labor, and Welfare of Japan. These sponsors had no role in the design of the study, the collection of the data, the analysis and interpretation of the data, the decision to submit the manuscript for publication, or the writing of the manuscript.

PML mediates glioblastoma resistance to mammalian target of rapamycin (mTOR)-targeted therapies

Akio Iwanami[a], Beatrice Gini[b,c,1], Ciro Zanca[b,1], Tomoo Matsutani[b], Alvaro Assuncao[d], Ali Nael[e], Julie Dang[f], Huijun Yang[b], Shaojun Zhu[g], Jun Kohyama[g], Issay Kitabayashi[h], Webster K. Cavenee[b,i], Timothy F. Cloughesy[j], Frank B. Furnari[b,i,k], Masaya Nakamura[a], Yoshiaki Toyama[a], Hideyuki Okano[l], and Paul S. Mischel[b,i,k,2]

Departments of [a]Orthopaedic Surgery and [l]Physiology, Keio University School of Medicine, Tokyo 160-8582, Japan; [b]Ludwig Institute for Cancer Research, [i]Moores Comprehensive Cancer Center, and [k]Department of Pathology, University of California at San Diego, La Jolla, CA 92093; [c]Department of Neurological, Neuropsychological, Morphological and Movement Sciences, University of Verona, 37134 Verona, Italy; [d]Undergraduate Minor in Biomedical Research Program, and Departments of [g]Molecular and Medical Pharmacology and [j]Neurology, University of California, Los Angeles, CA 90095; [e]Department of Pathology, University of California, Irvine, CA 92697; [f]School of Pharmacy, University of California, San Francisco, CA 94104; and [h]Division of Hematological Malignancy, National Cancer Center Research Institute, Tokyo 104-0045, Japan

Edited[†] by Joseph Schlessinger, Yale University School of Medicine, New Haven, CT, and approved February 1, 2013 (received for review October 12, 2012)

Despite their nearly universal activation of mammalian target of rapamycin (mTOR) signaling, glioblastomas (GBMs) are strikingly resistant to mTOR-targeted therapy. We analyzed GBM cell lines, patient-derived tumor cell cultures, and clinical samples from patients in phase 1 clinical trials, and find that the promyelocytic leukemia (PML) gene mediates resistance to mTOR-targeted therapies. Direct mTOR inhibitors and EGF receptor (EGFR) inhibitors that block downstream mTOR signaling promote nuclear PML expression in GBMs, and genetic overexpression and knockdown approaches demonstrate that PML prevents mTOR and EGFR inhibitor-dependent cell death. Low doses of the PML inhibitor, arsenic trioxide, abrogate PML expression and reverse mTOR kinase inhibitor resistance in vivo, thus markedly inhibiting tumor growth and promoting tumor cell death in mice. These results identify a unique role for PML in mTOR and EGFR inhibitor resistance and provide a strong rationale for a combination therapeutic strategy to overcome it.

mTORC1 | glioma

Glioblastoma (GBM) is the most common malignant primary brain tumor of adults and one of the most lethal forms of cancer (1, 2). As a consequence of frequent EGF receptor (EGFR) amplification and/or activating mutation, other receptor tyrosine kinase amplifications and phosphatase and tensin homolog (PTEN) loss (3, 4), persistent hyperactivation of the phosphatidyl-inositol-3-kinase (PI3K) pathway is observed in nearly 90% of GBMs making the downstream effector, mammalian target of rapamycin (mTOR), a compelling drug target. mTOR links growth factor signaling through PI3K to energy and nutrient status, protein translation, autophagy, and tumor cell metabolism (5). Thus, mTOR is a critical integrator that regulates tumor growth, survival and, potentially, cancer drug resistance.

The allosteric mTOR inhibitor rapamycin has failed in the clinic as a treatment for GBM patients. We previously reported that in a clinical phase I trial for patients with recurrent PTEN-deficient GBM, rapamycin treatment led to Akt activation resulting in loss of negative feedback, consistent with the homeostatic regulatory role of mTOR complex I (mTORC1) as a negative regulator of PI3K/Akt signaling (6). Further, we demonstrated a critical role for mTOR complex II (mTORC2) as a critical mediator of rapamycin resistance through Akt and mTORC1-independent signaling pathways (7). These results have highlighted the potential role for mTOR kinase inhibitors, which block both mTOR signaling complexes, in the treatment of GBM and potentially other cancers.

The interconnectivity between mTOR signaling complexes suggests the possibility that multiple mechanisms of mTOR inhibitor resistance may exist, some of which may be clinically actionable. The promyelocytic leukemia (PML) gene may represent one such mechanism. PML is a pleiotropic tumor suppressor that plays multiple roles on cellular homeostasis such as apoptosis, proliferation, and senescence (8, 9). PML, as part of the retinoic acid receptor (RAR)/PML fusion protein identified in acute promyelocytic leukemia, represents one of the first molecular cancer targets amenable to targeted drug therapy (10, 11). Although the loss of PML protein expression is associated with tumor progression in many tumors (12), some tumors show paradoxically high levels of PML. For example, PML has been shown to be highly expressed in hematopoetic stem cells and in chemotherapy resistant, quiescent leukemia-initiating CML cells (13).

PML is also closely related to receptor tyrosine kinase (RTK)/PI3K/Akt/mTOR signaling pathway at multiple levels. PML has been reported to oppose the function of nuclear Akt (14) and was also identified as a repressor of mTOR through inhibition of Ras homolog enriched in brain (Rheb)–mTOR interaction during hypoxia (15). Further, PML is responsible for the repression of transcriptional activity from the EGFR promoter (16). Considering these factors, we hypothesized that PML might promote resistance to rapamycin, ATP-competitive mTOR kinase inhibitors, and EGFR tyrosine kinase inhibitors by controlling RTK/PI3K/Akt/mTOR signaling and cell cycle in GBM. Here, we examine the expression of PML in GBM cell lines and GBM-patient tissues; show that it is regulated by PI3K/Akt/mTOR signaling; demonstrate the impact of mTOR inhibition on PML expression; and then, using genetic and pharmacological approaches and correlations from clinical samples of patients treated with rapamycin or erlotinib, demonstrate a role for PML in preventing drug-induced apopotosis and promoting clinical resistance. Finally, we identify genetic and pharmacological approaches to overcome this drug resistance.

Results

PML Expression in GBM Patients. To examine the expression of PML in GBM patients, we performed immunohistochemical analysis of GBM by using a tissue microarray (TMA) consisting of multiple representative regions of tumor and adjacent normal tissue from 87 patients with primary GBMs (17, 18). Expression of PML, Ki-67, and phospho-S6 was analyzed and scored independently by two neuropathologists as high or low (scoring summarized in Fig. 1 *A* and *B*). PML was highly expressed in 41.4% of tumor samples (Fig. 1 *A* and *B*), and the expression was

Author contributions: A.I., B.G., C.Z., W.K.C., T.F.C., F.B.F., and P.S.M. designed research; A.I., B.G., C.Z., T.M., A.A., A.N., J.D., H.Y., S.Z., and J.K. performed research; C.Z., T.M., I.K., and F.B.F. contributed new reagents/analytic tools; A.I., B.G., C.Z., T.M., W.K.C., T.F.C., F.B.F., M.N., Y.T., H.O., and P.S.M. analyzed data; and A.I., B.G., C.Z., T.M., W.K.C., T.F.C., F.B.F., M.N., Y.T., H.O., and P.S.M. wrote the paper.

The authors declare no conflict of interest.

[†]This Direct Submission article had a prearranged editor.

Freely available online through the PNAS open access option.

[1]B.G. and C.Z. contributed equally to this work.

[2]To whom correspondence should be addressed. E-mail: pmischel@ucsd.edu.

This article contains supporting information online at www.pnas.org/lookup/suppl/doi:10.1073/pnas.1217602110/-/DCSupplemental.

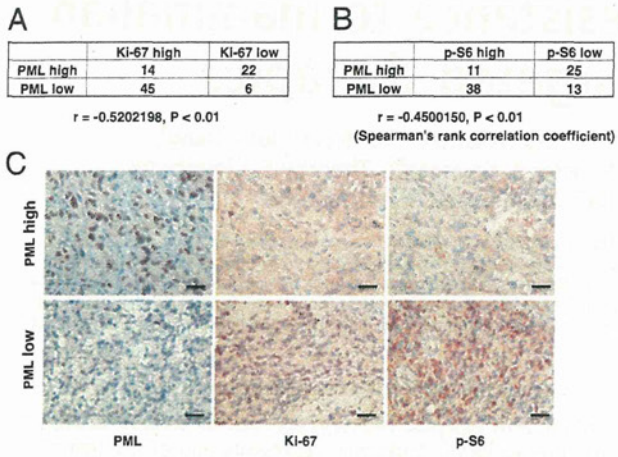

Fig. 1. PML is inversely correlated with proliferation rate and mTOR signaling in GBM clinical samples. (*A* and *B*) Tissue microarrays containing tumor samples from 87 GBM patients were stained by using PML, Ki-67, and p-S6 antibody, respectively. PML is highly expressed in 40% of GBM patients. Correlation analyses show PML significantly inversely correlate with Ki-67 (*A*) and p-S6 (*B*). (*C*) Immunohistochemical staining of (reddish brown) PML, Ki-67, and p-S6 from a representative GBM patient. (Magnification: 10×.) Nuclei were counterstained with hematoxylin (blue). (Scale bar: 100 μm.)

significantly inversely correlated with the cell proliferation marker Ki-67 (Fig. 1 *A* and *C*; $r = -0.52$, $P < 0.01$) and with mTORC1 signaling, as measured by S6 phosphorylation (Fig. 1 *B* and *C*; $r = -0.45$, $P < 0.01$).

Rapamycin Induces Expression and Nuclear Aggregation of PML. Next, we treated GBM cells and a GBM patient-derived cell culture with rapamycin to determine the effect of RTK/PI3K/mTOR inhibitor on PML (Fig. 2 *A–C*). Exposure to rapamycin treatment, or the ATP-competitive mTOR kinase inhibitor pp242, at doses sufficient to inhibit mTORC1 signaling, led to time-dependent increases in PML expression (Fig. 2 and Fig. S1). The EGFR tyrosine kinase inhibitor, erlotinib, which inhibited mTORC1 signaling downstream of EGFR, similarly elevated PML expression (Fig. 2*B*). Biochemical results were confirmed by fluorescent immunocytochemical analyses, demonstrating strongly granular patterns of PML staining in the nucleus, consistent with its reported distribution (Fig. 2*C*).

Overexpression of PML Contributes to Decreasing PI3K/Akt/mTOR Signaling and a Slower Cell Cycle. We hypothesized that PML might contribute to rapamycin, mTOR kinase inhibitor, and/or EGFR tyrosine kinase inhibitor resistance in GBM. Therefore, we performed retroviral transduction of PML I into U87 cells and examined the effect on PI3K/Akt/mTOR signaling and cell cycle progression. First, we performed double-immunofluorescent staining with PML and HA tag to confirm the overexpression of PML I (Fig. 3*A*). Compared with control, the retroviral-infected U87 cells expressed exogenous PML in both their nuclei and cytoplasm. Immunoblot analyses of these lysates demonstrated the increased expression of all PML isoforms, which would result from alternative splicing of the longest form, PML I (9). After confirmation of PML overexpression in these cell lines, we examined several PI3K/Akt/mTOR signaling proteins and cell cycle-related proteins by Western blotting. Akt and S6 phosphorylation were significantly decreased in U87 GBM cells that exogenously expressed PML I. Moreover, the cell cycle related proteins, cyclin D1 and cyclin-dependent kinase inhibitor 1 (p21), were also notably decreased, suggesting that PML contributes to decreasing PI3K/Akt/mTOR signaling and slowing down the cell cycle (Fig. 3*B*). We further performed cell proliferation assays by using these cell lines and confirmed that U87PML I cells were significantly less proliferative than control U87 cells (Fig. 3*C*; $^{**}P < 0.01$).

Flow cytometric cell cycle analyses demonstrated an increased G1 fraction in U87PML I-expressing GBM cells (Fig. 3*D*; $^{**}P < 0.01$). To determine whether this conferred rapamycin resistance, we treated U87PML I cells and control cells with rapamycin for 48 h and analyzed the drug effect by using WST-1 assays. PML I overexpression significantly reduced the growth inhibitory effect of rapamycin (Fig. 3*E*; $^{**}P < 0.01$).

Interfering RNA-Mediated PML Knockdown Sensitizes GBM Cell Lines to mTOR and EGFR Kinase Inhibitor Treatment. To confirm a specific role for PML in preventing mTOR and EGFR-kinase inhibitor-dependent cell death, we induced small interfering RNAs (siRNA)-mediated PML knockdown in multiple GBM cell lines and assessed its impact on response to rapamycin, pp242, and erlotinib. TUNEL analysis demonstrated that PML knockdown significantly sensitized all of the GBM cell lines to pp242 and erlotinib-mediated cell death (Fig. 4 *A* and *B*; $^{*}P < 0.05$, $^{**}P < 0.01$), which was confirmed by analysis of polyADP ribose polymerase (PARP) cleavage (Fig. S2). Of note, in contrast to pp242, rapamycin, which has less activity against mTORC2 than does pp242, induced minimal cell death even in the presence of PML knockdown, potentially suggesting a role for sustained mTORC2 signaling in mediating survival (7). Taken together, these data demonstrate that PML contributes to mTOR and EGFR kinase inhibitor resistance in GBM by suppressing tumor cell death, which can be reversed by pharmacological or genetic inhibition of PML.

As_2O_3 Abrogates pp242-Induced PML Up-Regulation and Sensitizes GBMs to mTOR Kinase Inhibitor-Mediated Cell Death. Arsenic trioxide (As_2O_3) has long been used as a therapeutic agent for promyelocytic leukemia (19–21). Besides its cell toxicity, As_2O_3 has been shown to target PML for degradation through a sumoylation-dependent process leading to PML polyubiquitination and proteosomal degradation (11, 13, 22–24). Therefore, we investigated the effect of As_2O_3 on reduction of PML in U87 cells. Single As_2O_3 treatments reduced PML expression at both low (0.15 μM) and high concentrations (2 μM) and decreased proliferation in serum-containing growth condition (Fig. S3 *A* and *B*). Notably, a high concentration (2 μM) induced an increase in p53 levels and decreased levels of cyclin D1 expression (Fig. S3*A*). The ability of low dose As_2O_3 to inhibit proliferation in the absence of p53 induction is consistent with previous papers (13, 25)

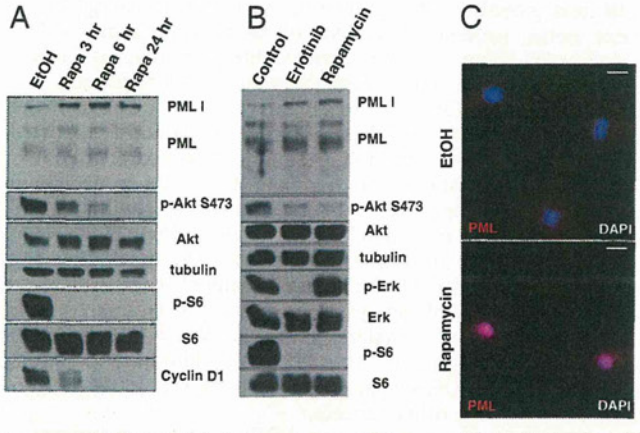

Fig. 2. PI3K/Akt/mTOR inhibitors induce PML expression in GBM cells. (*A*) Western blot analysis of the effect of rapamycin treatment on PML expression in U87 cells. Cells are cultured in serum-free condition. (*B*) Effect of the EGFR inhibitor erlotinib and rapamycin on PML expression in GBM patient-derived cells. Cells are cultured under neurosphere conditions. (*C*) Immunofluorescence of PML (red) in U87 cells treated with rapamycin or control. Nuclei are stained with DAPI (blue). (Scale bar: 20 μm.)

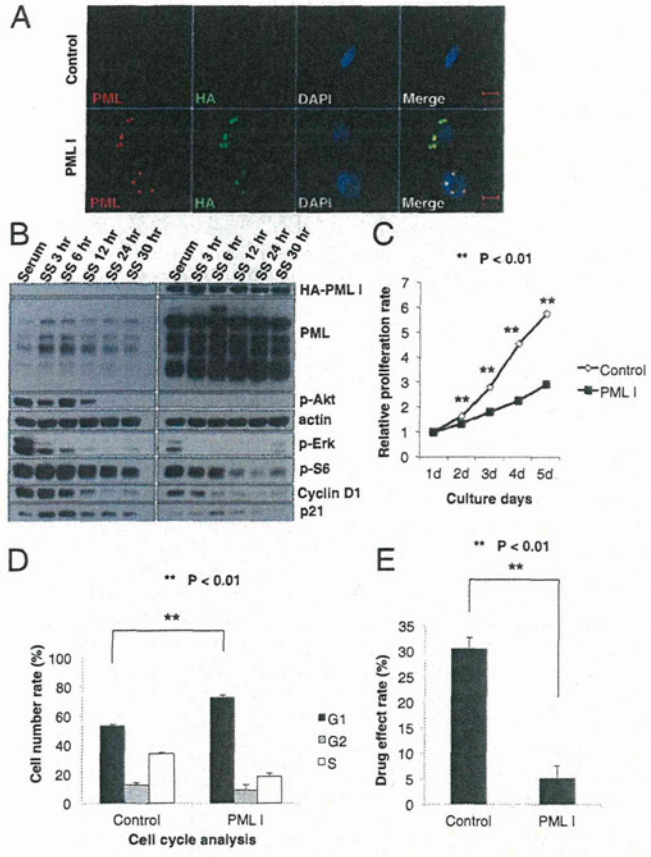

Fig. 3. PML overexpression decreases PI3K/Akt/mTOR signaling and slows down cell cycle. (*A*) Immunofluorescence in U87 control or hemagglutanin-tagged PML1 (HA-PMLI) infected cells. (Scale bar: 10 μm.) (*B*) Western blot analysis of PI3K/Akt/mTOR signaling pathway and cell cycle-related proteins performed on lysates from U87 control or HA-PMLI infected cells. Cells were placed in serum-free medium, cultured, and collected in each time course. (*C*) Proliferation of U87 control and HA-PMLI infected cells analyzed by WST assay. *P* value was determined by Student's *t* test. (*D*) Effect of PMLI overexpression on cell cycle progression in U87 cells. Cell cycle distribution was performed by flow cytometric analysis. *P* value was determined by Student's *t* test. (*E*) Effect of treatment with rapamycin on growth of U87 control and HA-PMLI infected cells analyzed by WST assay. *P* value was determined by Student's *t* test.

suggesting that lower concentration of As_2O_3 mediates its effect by reducing PML levels and not by inducing DNA damage. Neither pp242, nor As_2O_3 alone, promoted extensive tumor cell death. In contrast, As_2O_3 (0.15 μM) significantly and synergistically promoted pp242- dependent apoptotic cell death, as measured by cleaved caspase and TUNEL staining, independent of any effect on p53 phosphorylation (*$P < 0.01$; Fig. 5 *A* and *B* and Fig. S3*C*).

Therefore, we analyzed the effect of combining the mTOR kinase inhibitor pp242 with As_2O_3 on PML expression, cell death, and tumor size in U87 GBM xenografts (Fig. 5 *C–F*). Sixteen days of treatment with pp242 and As_2O_3, significantly reduced the growth of GBMs by nearly threefold ($P < 0.0005$) and induced TUNEL-positive cell death, an effect that was not detected with either pp242 or As_2O_3 monotherapy (Fig. 5 *C, D,* and *F*). Importantly, As_2O_3 also abrogated the pp242-mediated up-regulation of PML expression (Fig. 5*E*). Ki-67 staining was also diminished, although the decrease failed to reach statistical significance (Fig. S4). Taken together, these results demonstrate that As_2O_3 dramatically synergizes with mTOR kinase inhibition to promote GBM cell death and block tumor growth in vivo.

Immunohistochemical Analyses of PML Expression in GBM Patients Treated with Rapamycin or Erlotinib. Finally, to establish clinical relevance and to determine whether PML up-regulation is associated with mTOR and EGFR inhibitor resistance in GBM patients, we performed immunohistochemical analyses of tumor samples obtained from two "biopsy-treat-biopsy" paradigm phase I clinical trials, for which tumor tissue was obtained 7–10 d after treatment with rapamycin or lapatinib (details presented in refs. 6 and 26). As shown in Fig. 6, rapamycin (Fig. 6 *A* and *B*) and erlotinib (Fig. 6 *C* and *D*) treatment were both associated with significantly enhanced nuclear PML expression (*$P < 0.01$).

Discussion

PML is a pleiotropic tumor suppressor protein that is lost in many cancer types (12, 27). PML negatively regulates Akt-mTOR signaling (14, 28) and suppresses PTEN loss- induced prostate tumorigenesis (14) and mTOR-dependent renal carcinoma progression (28). We provide evidence from preclinical models and in patients that PML suppresses Akt/mTOR signaling and proliferation (Fig. 1). However, PML is also commonly overexpressed in cancer, including in GBM (12, 29), and has been shown to promote a range of activities that may enhance the growth and progression of cancer, including oncogene-induced senescence (29), hematopoetic stem cell maintenance, and breast cancer tumor cell survival through a peroxisome

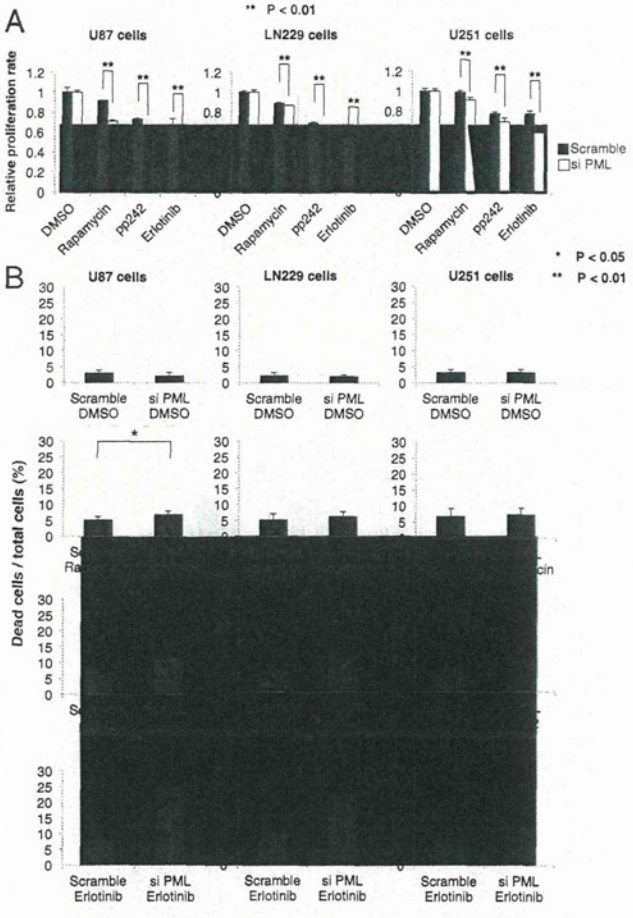

Fig. 4. PML knockdown sensitizes GBM cell lines to EGFR and mTOR targeted therapies. (*A*) Cell viability assays demonstrate a synergistic effect of PML knockdown and each indicated inhibitor. *P* values were determined by Student's *t* test. (*B*) Effect of PML knockdown and each indicated inhibitor on multiple GBM cell lines analyzed by Trypan blue exclusion. *P* values were determined by Student's *t* test.

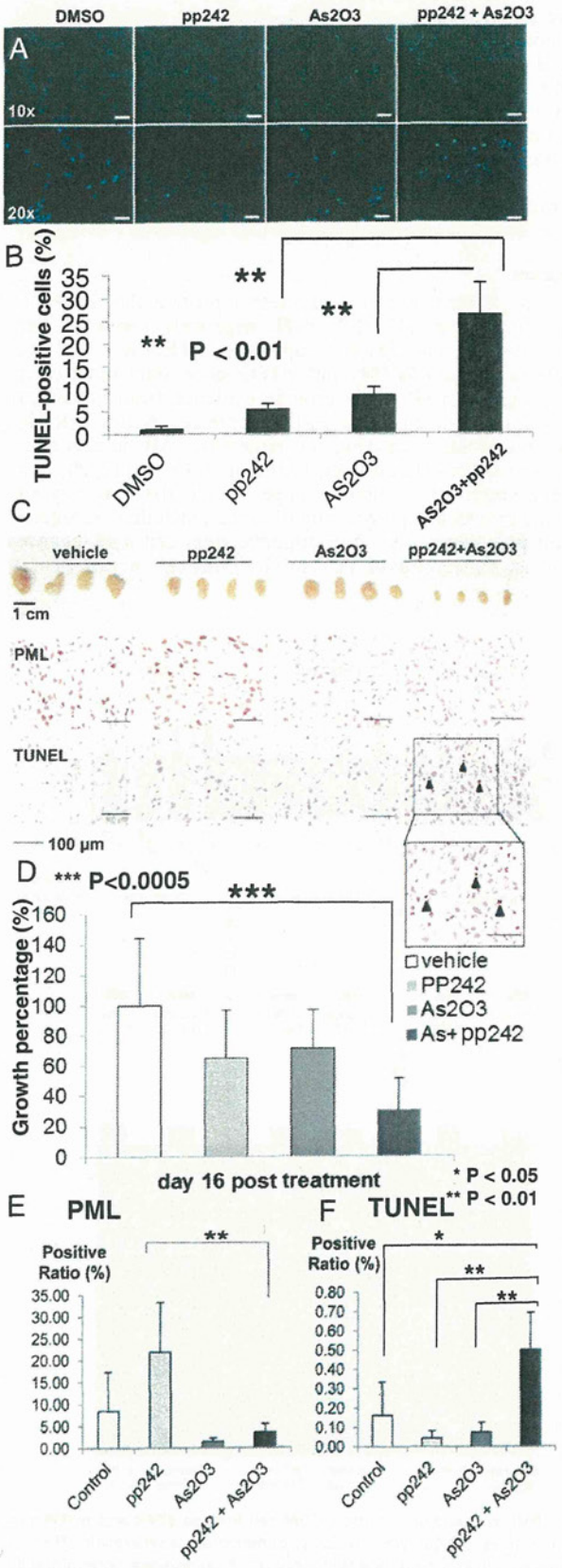

Fig. 5. As_2O_3 reduces PML and sensitizes GBM cells to mTOR-targeted therapies. (*A*) Representative images demonstrating TUNEL staining (green) to assess apoptotic effect of pp242 and As_2O_3 (2 μM) on U87 cells in vitro. Nuclei are stained blue. (*B*) Quantification of TUNEL staining. *P* values were determined by Student's *t* test. (*C*) Representative photographs of U87 GBM xenografts treated daily with vehicle, pp242 (60 mg/kg per day by oral gavage), As_2O_3 (2.5 mg/kg intraperitoneally), or combination (n = 8 mice per condition). Images of representative PML and TUNEL stains. (*D*) Quantification demonstrating greater than threefold reduction in tumor size for mice treated with combined pp242 and As_2O_3 ($P < 0.005$). (*E* and *F*) Quantification of PML and TUNEL xenograft tumor staining from each treatment conditions.

proliferator-activated receptor (PPAR)-γ/fatty acid oxidation-dependent pathway (30, 31). Further, PML has been shown to mediate resistance of leukemias to chemotherapy by supporting maintenance of a "quiescent" tumor cell population (13). Its impact on cancer drug resistance, including drugs that target mTOR or its upstream effectors, in solid tumors including GBM is less clear. Through integration of preclinical studies with analysis of tumor tissue from patients in phase I clinical trials, we demonstrate an important role for PML in mediating mTOR and EGFR inhibitor resistance in GBM. These results present evidence that mTOR inhibition promotes PML up-regulation in patients and that this up-regulation of PML mediates drug resistance.

It is tempting to speculate that PML promotes this resistance by inducing a "quiescent state" through inhibition of Akt/mTOR signaling. However, we cannot formally exclude the possibility that PML may drive resistance through its metabolic prosurvival effects. In fact, this possibility is consistent with our previous observation that EGFR mutant GBMs have enhanced reliance on fatty acid synthesis for survival (17), creating enhanced dependence on fatty acid oxidation for survival (32). Futures studies will be needed to determine the mechanisms by which PML promotes drug resistance in GBM.

mTOR has emerged as a critical target in GBM because it is persistently hyperactivated downstream of the most common GBM alterations including EGFR amplification, EGFR variant III (EGFRvIII) mutation, platelet-derived growth factor receptor (PDGFRα) and hepatocyte growth factor receptor (c-MET) amplification, and PTEN loss (3). We have demonstrated that mTOR inhibition is required for the efficacy of EGFR-targeted therapies (33), suggesting a mechanistic basis by which EGFR tyrosine kinase inhibitors (TKIs) may also potently up-regulate PML expression to promote drug resistance. For both EGFR TKIs and mTOR kinase inhibitors, the potential for converting a cytostatic response, which often yields minimal benefit, to a cytotoxic response by pharmacologically abrogating PML, could potentially represent a significant clinical advance. Our demonstration of a synergism between the two classes of compound in cell death induction underscores this possibility.

Pharmacologically targeting PML represents one of the most exciting success stories for the principle of molecularly guided therapies (10, 11). As_2O_3 targets PML for degradation through a SUMOylation-dependent process (34), potently promoting long-term remission in patients and mice with acute promyelocytic leukemia bearing the PML/RAR fusion (24). Its role in solid cancers has yet to be established. However, As_2O_3 given with standard chemotherapy can be tolerated by GBM patients, as demonstrated in recent clinical trials (35). The results presented here suggest a clinically actionable strategy to combine resistance by combining As_2O_3 with mTOR kinase and EGFR TKIs for the treatment of GBM patients.

Materials and Methods

Cell Lines. U87, LN229, and U251 GBM cell lines were cultured as previously described (18, 26). Brain tumor samples were collected after surgical resection under University of California, Los Angeles (UCLA) institutional review board-approved protocols between 1999 and 2011 from patients who gave informed consent, and graded by the neuropathologist in accordance with World Health Organization-established guidelines. Neurosphere cultures were prepared as described (36). Full details are provided in *SI Materials and Methods*.

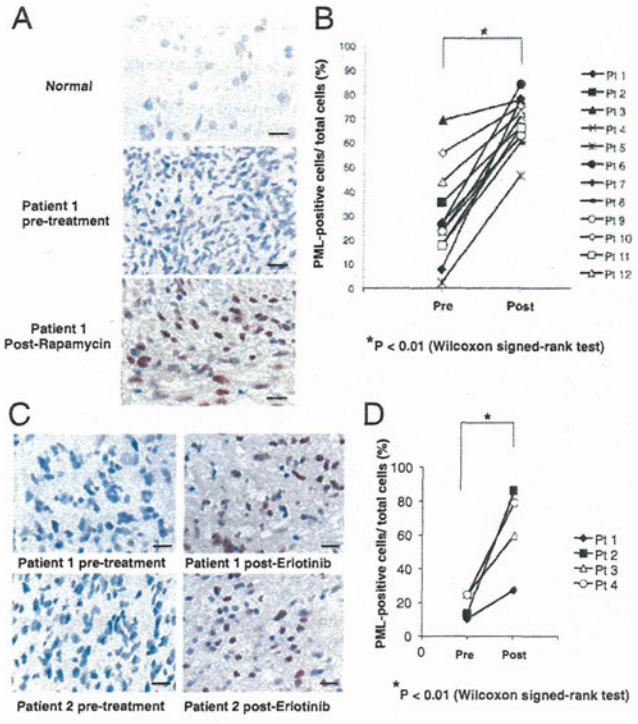

Fig. 6. Rapamycin and erlotinib treatment induces PML expression in GBM patient tumor tissues. (*A*) Immunohistochemical staining (reddish brown) of PML before and after treatment with rapamycin. Nuclei were counterstained with hematoxylin (blue). (*B*) Quantification of immunohistochemical staining from >1,000 cells from at least three representative areas of each tumor before and after rapamycin treatment. *P* value was determined by Wilcoxon signed-rank test. (*C*) Immunohistochemical staining (reddish brown) of PML before and after treatment with erlotinib. Nuclei were counterstained with hematoxylin (blue). (*D*) Quantification of immunohistochemical staining from >1,000 cells from at least three representative areas of each tumor before and after erlotinib treatment. *P* value was determined by Wilcoxon signed-rank test. (Scale bars: 50 μm.) (Magnification: 20×.)

Antibodies and Reagents. We used antibodies directed against the following: phosopho-Akt Ser473, Akt, phospho-S6 Ser235/236, S6, phospho-Erk, Erk, CyclinD1, cleaved PARP (Cell Signaling); β-actin, p21 (Sigma); phospho-EGFR Tyr1086 (Invitrogen); EGFR (Millipore); PML (for Western blotting, Abcam; for immunohistochemisry, Santa Cruz). Reagents used are rapamycin, As_2O_3, polybrene (Sigma), erlotinib (ChemieTex), pp242 (Chemdea). Full details of immunoblot analysis are provided in *SI Materials and Methods*. Stock solutions of inhibitor for rapamycin were made by dissolving in ethanol, erlotinib, and pp242 were made by dissolving in DMSO (Sigma) and stored at −20 °C. Inhibitors were added to each well at final concentrations of 10 nM, 10 μM, and 2 μM, respectively. An equal concentration of ethanol or DMSO served as control. As_2O_3 was diluted by PBS and 10 M NaOH, then pH was adjusted at 8.0 by 12 M HCl.

Plasmid, Retroviral Infection, and siRNA Transfection. Plasmid 22(pLNCX) encoding hemagglutinin (HA) tag-expression construct was obtained from the I.K. laboratory (37). Full details are available in *SI Materials and Methods*. Transfection of siRNA into GBM cell lines was carried out by using Lipofectamine RNAiMAX (Invitrogen) in full serum, with medium change after 24 h. On-TARGET plus SMARTpool siRNAs (Dharmacon) specifically targeting PML (catalog no. L-006547-000005) and nontargeting control pools of siRNAs (catalog no. D-0018-10-10-05) were used at 10 nM, and cells were harvested 48 h after transfection.

Cell Proliferation and Death Assays. Relative proliferation to control cells with vehicle treatment was checked with a WST-1 Cell Proliferation Assay Kit (Millipore). Cell death was assessed by Trypan blue exclusion (Invitrogen). Full details are given in *SI Materials and Methods*.

Cell Cycle Analyses. Cells were fixed in 70% ethanol diluted in PBS, and the samples were stored at −20 °C. The fixed cells were resuspended in PBS containing 20 μg/mL propidium iodide (Sigma) and 10 μg/mL RNase A (Sigma), and incubated for 10 min at 37 °C. Flow cytometric analysis was performed by using FACSCalibur flow cytometer (Becton Dickinson).

TUNEL Staining and Immunofluorescence Analysis. For TUNEL staining, cells were placed in eight-well chamber slides, incubated with TUNEL Reaction Mixture (Roche) at 37 °C for1 h in the dark, and visualized with a fluorescene microscope (Olympus BX-61). Ten separate, randomly chosen fields on each chamber were imaged, and the numbers of TUNEL-positive cells and whole nuclei were counted. For immunofluorescence analysis with indicated antibodies, cells were fixed with 4% paraformaldehyde in PBS for 10 min, washed twice in PBS, incubated with primary antibodies in PBS containing 3% BSA at 4 °C overnight, and detected with appropriate fluorescence-conjugated secondary antibodies. Full details are presented in *SI Materials and Methods*.

In Vivo Studies. We suspend 1.25×10^6 U87 GBM cells in 100 μL of Matrigel, PBS 1:2 solution, and injected them subcutaneously into the right flank of each 4- to 5-wk-old athymic nude mice. Tumors were measured with an electronic caliper, and volumes were calculated by using width (*a*), length (*b*), and depth (*c*) measurements ($V = a \times b \times c$). Ten days after injection, mice were treated daily with vehicle, 60 mg/kg pp242 by gavage, 2.5 mg/kg intraperitoneally injected As_2O_3 or their combination, respectively. Mice were euthanized when tumor volume of treated mice reached statistical significance compared with control groups. Mice were euthanized in accordance with the University of California at San Diego Institutional Guidelines for Animal Welfare and Experimental Conduct.

Immunohistochemical Assays, Tissue Microarrays, and Image Analysis-Based Scoring. Immunohistochemical staining and analysis of two GBM TMAs was performed, as described (6, 26). Among 140 cases, 87 GBM patient tissue cores were available for analysis based on sufficient high quality tissue. Staining intensity was scored independently by two pathologists who were unaware of the findings of the molecular analyses. See *SI Materials and Methods* for full details.

Statistical Analysis. Results are shown as mean ± SEM. χ^2 for independence test was used to assess correlations between various molecular markers on TMAs. For nonparametric clinical trial data, Wilcoxon rank test was used. Other comparisons in cell proliferation assays, cell death assays, and TUNEL staining were performed with Student's *t* test, as by analysis of variance, appropriate. $P < 0.05$ was considered as statistically significant.

ACKNOWLEDGMENTS. We thank Dr. George Thomas for helpful discussions and comments on this paper. A.I. and J.K. were supported in part by a grant from the Japan Society for the Promotion of Science. A.I. was also supported by a grant from the Uehara Memorial Foundation. B.G. is supported by a Marie Curie Fellowship from the European Commission- PIOF-GA-2010-271819. C.Z. is supported by an American-Italian Cancer Foundation post-doctoral research fellowship. This work was supported by National Institutes of Health (NIH) Grants NS73831 and CA119347 (to P.S.M.), by the Ziering Famiy Foundation in memory of Sigi Zeiring (P.S.M. and T.F.C.), the Ben and Catherine Ivy Foundation (P.S.M. and T.F.C.), and NIH Grant P01-CA95616 (to W.K.C.). W.K.C. is a Fellow of the National Foundation for Cancer Research.

1. Furnari FB, et al. (2007) Malignant astrocytic glioma: Genetics, biology, and paths to treatment. *Genes Dev* 21(21):2683–2710.
2. Wen PY, Kesari S (2008) Malignant gliomas in adults. *N Engl J Med* 359(5):492–507.
3. Anonymous; Cancer Genome Atlas Research Network (2008) Comprehensive genomic characterization defines human glioblastoma genes and core pathways. *Nature* 455(7216):1061–1068.
4. Parsons DW, et al. (2008) An integrated genomic analysis of human glioblastoma multiforme. *Science* 321(5897):1807–1812.
5. Yecies JL, Manning BD (2011) Transcriptional control of cellular metabolism by mTOR signaling. *Cancer Res* 71(8):2815–2820.
6. Cloughesy TF, et al. (2008) Antitumor activity of rapamycin in a Phase I trial for patients with recurrent PTEN-deficient glioblastoma. *PLoS Med* 5(1):e8.
7. Tanaka K, et al. (2011) Oncogenic EGFR signaling activates an mTORC2-NF-κB pathway that promotes chemotherapy resistance. *Cancer Discov* 1(6):524–538.
8. Bernardi R, Pandolfi PP (2003) Role of PML and the PML-nuclear body in the control of programmed cell death. *Oncogene* 22(56):9048–9057.
9. Bernardi R, Pandolfi PP (2007) Structure, dynamics and functions of promyelocytic leukaemia nuclear bodies. *Nat Rev Mol Cell Biol* 8(12):1006–1016.
10. Andre C, et al. (1996) The PML and PML/RARalpha domains: From autoimmunity to molecular oncology and from retinoic acid to arsenic. *Exp Cell Res* 229(2):253–260.